USE OF HYDROXYAPATITE DERIVED FROM CATFISH BONES FOR

REMEDIATING URANIUM CONTAMINATED GROUNDWATER

Except where reference is made to the work of others, the work described in this thesis is my own or was done in collaboration with my advisory committee. This thesis does not include proprietary or classified information.

_____

Shyamsundar Ayalur Chattanathan

Certificate of Approval:

_____	_____
Mark O. Barnett Associate Professor Civil Engineering	T. Prabhakar Clement, Chair Professor Civil Engineering
_____	_____
Xing Fang Associate Professor Civil Engineering	George T. Flowers Dean Graduate School

USE OF HYDROXYAPATITE DERIVED FROM CATFISH BONES FOR REMEDIATING URANIUM CONTAMINATED GROUNDWATER

Shyamsundar Ayalur Chattanathan

A Thesis

Submitted to

the Graduate Faculty of

Auburn University

in Partial fulfillment of the

requirements for the

degree of

Master of Science

Auburn, Alabama

August 10, 2009

USE OF HYDROXYAPATITE DERIVED FROM CATFISH BONES FOR

REMEDIATING URANIUM CONTAMINATED GROUNDWATER

Shyamsundar Ayalur Chattanathan

Permission is granted to Auburn University to make copies of this thesis at its discretion, upon the request of individuals or institutions and at their expense. The author reserves all publication rights.

_____

Signature of Author

_____

Date of Graduation

VITA

Shyamsundar A.C, son of A.R. Chattanathan and R.Banumathi was born on April 13, 1986, in Chennai, India. He graduated from D.A.V. school, Chennai, India in April 2003. In May 2007, he graduated from Sri Venkateswara College of Engineering, Sriperumbudur, Chennai, India with a Bachelor's degree in Chemical Engineering. He entered the graduate school at Auburn University in Fall 2007 to pursue his Master of Science degree in the field of Environmental Engineering, in the Department of Civil Engineering.

THESIS ABSTRACT

USE OF HYDROXYAPATITE DERIVED FROM CATFISH BONES FOR REMEDIATING URANIUM CONTAMINATED GROUNDWATER

Shyamsundar Ayalur Chattanathan

Master of Science, August 10, 2009

(B.S. Sri Venkateswara College of Engineering, Chennai, India, 2007)

73 Typed Pages

Directed by T. Prabhakar Clement

Hydroxyapatite derived from catfish bones was used for removing uranium from contaminated groundwater. Literature review indicated that apatites from various sources of fish bones can be used for metal remediation. The significance of this study is that apatite prepared from the bones of catfish was used to study uranium removal processes. Since the organic material associated with the fish bones are known to hinder the sorption process, they were systematically removed through mechanical and chemical treatment before using them in the experiments. The catfish bones were further subjected to thermal

treatment at 100°C and 300°C. The catfish hydroxyapatite (CFHA) prepared at a lower temperature was found to be the most effective reactant and hence was selected for further studies. Thermally treated catfish bones were characterized using XRD and SEM techniques and the presence of hydroxyapatite was confirmed. Multiple pH edge experiments were performed to understand the variation of uranium removal capacities with changes in pH, and the data showed that the maximum sorption occurred between pH 5 to 8.5. The effect of particle size on uranium adsorption was investigated using three different sizes of CFHA: large (> 2000 μ), medium (2000 μ-300 μ), and small (<300 μ). Batch sorption experiments were completed using these three CFHA particles to understand the role of particle size and surface area on sorption capabilities. The results indicated that the smallest particles exhibited high removal efficiency (of about 18 mg of U/g CFHA). Column experiments were completed using the smallest CFHA particles at different flow rates and breakthrough profiles were obtained. The scalability of the adsorption reaction was tested using different column experiments. First, a column experiment was performed using a fixed amount of sorbent using 1 ppm uranium solution. Later, breakthrough profiles were obtained by doubling both the amount of sorbent in the column and the inlet concentration. The results indicated that both the breakthrough curves followed a similar trend indicating the scalability of adsorption to the sorbent mass. Mass balance closure was verified for both batch and column data. The results indicated that the mass balance error was ~20% and ~10% for batch and column experiments, respectively. The results of this research indicate that CFHA is an effective sorbent and can be potentially used in permeable reactive barriers for treating uranium plumes.

ACKNOWLEDGMENTS

First of all, I would like to express my gratitude to Dr. Prabhakar Clement for his sincere efforts in not only reviewing this thesis thoroughly but also in guiding me throughout the masters program. I would like to dedicate this thesis to Dr. Clement for his constant support without which the thesis would not have taken this form. Thanks to the committee members Dr. Xing Fang and Dr. Mark Barnett for reviewing the thesis. Special thanks to Dr. Mark Barnett for allowing me to work in his lab during my masters program. This work was supported by U.S. Department of Energy Grant No. DE-FG02-06ER64213 at Auburn University. We acknowledge the support provided by Dr Nagraj Chatakundi for obtaining the catfish bones.

I would like to express my appreciation to my office and lab mates: Vijay, Gautham, Sushil Kanel, Jagadish, Gopal, Anand, and Sun woo who made an interesting and competitive work environment. I am immensely thankful to my parents, and sister (Chithra) for their constant encouragement and support. Finally, thanks to Auburn University and the entire staff of the Department of Civil Engineering. Thank you.

Style manual or journal used Science of Total Environment.

Computer software used Microsoft Office 2007 (Microsoft Word, Microsoft Excel), Endnote 9.0.

TABLE OF CONTENTS

LIST OF FIGURES.....xii

CHAPTER

I. INTRODUCTION……..……..……....…1

1.1.Background……..……...……..…….……1

1.2.Objectives……...……..……...…..…. 6

1.3 Organization of Thesis……..…..…..……7

II. LITERATURE REVIEW…….....…….....…..... 9

2.1 Mechanism of metal sequestration within apatite…….……...… 10

2.2 Apatite from natural sources…….……..……...… ...12

2.3 Fish Bone Ceramic…….…….. ...13

2.4 Effect of Organics……..……..……14

2.5 HAP and Fish bone apatite as PRB……. 15

2.6 Removal efficiencies…..……. 16

2.7 Factors affecting sorption on Hydroxyapatite.……..……...….. .17

2.8 Column Experiments using Hydroxyapatite ……..……...…...18

2.9 Fish bone as a substitute for Hydroxyapatite ……...……...18

III. USE OF HYDROXYAPATITE DERIVED FROM CATFISH BONES FOR REMEDIATING URANIUM CONTAMINATED GROUNDWATER….....19

3.1 Material and Methods…….……20

3.2 Design of the batch experiment ……...……..20

3.3 Design of the column experiment …….…....21

3.4 Results and Discussion ……..…... .23

3.5 Effect of pH …….….. .24

3.6 Effect of preparation temperature on uranium removal kinetics……...…26

3.7 Effect of Particle size of catfish bone on uranium removal ……..... ..28

3.8 Comparison of CFHA Kinetics with CHA Kinetic at different pH values ……..… ..32

3.9 U(VI) Adsorption Isotherms ..……....33

3.10 Column experiment to study the effect of particle size on U(IV) removal..... 36

3.11 Effect of flow rate ….....……...39

3.12 Testing the Scalability of U(IV) Removal Processes …….....…....……..….... ..41

3.13 Column performance at pH 7 …….....……..…. .42

3.14 Verifying mass balance closure of batch and column data……44

IV. CONCLUSIONS AND RECOMMENDATIONS.....……..……...46

REFERENCES……...…….…….....49

APPENDIX - I……...…… 55

APPENDIX – II..... 59

LIST OF FIGURES

Figure 1: Uranium concentration across USA in rocks and surface soil……..…….…….3

Figure 2 : Typical column setup used in the study ……... 21

Figure 3 : SEM image of commercial HA and CFHA ……..... 23

Figure 4 : Comparison of XRD of fish bone HA and commercial HA…....……... .24

Figure 5 : Influence of pH on sorption of U(VI) onto commercial hydroxyapatite and fish bone……26

Figure 6 : Images of fish bone heated at two different temperatures …..…….… 27

Figure 7 : Effects of CFHA preparation temperature on the kinetics of uranium removal process ……...……28

Figure 8a : Image of fish bone hydroxyapatite with different particle sizes ……..…..… 29

Figure 8b : Depiction of increase in surface area with reduction in particle size .....…....30

Figure 9 : Effects of CFHA particle size on the kinetics of uranium removal process … 31

Figure 10 : Comparison of uranium removal kinetics using CFHA and CHA ……33

Figure 11 : Isotherm data for CFHA at pH 7…….....35

Figure 12 : Isotherm data for CFHA at pH 8.5 and 9….....……..…..36

Figure 13 : Column data- Effects of particle size on breakthrough concentrations ..…... .38

Figure 14 : Column data- Effects of flow rates …….40

Figure 15 : Scalability of observed breakthrough data at pH 8.5 …….. 42

Figure 16 : Column Break through data at pH 7 ……..44

CHAPTER 1

INTRODUCTION

1.1 Background

About 98% of the freshwater resources available for human use are in the form of groundwater (Fetter, 1988). With growing population, the demand for groundwater has been constantly going up every year. Also, due to rapid industrial growth, groundwater aquifers at many sites have been contaminated with various contaminants including heavy metals, ions, radionuclide, and microorganisms. Nuclear industry, for example, has experienced rapid growth in recent years since several nuclear power plants have come on-line throughout the world. The nuclear wastes discharged from these plants are major causes of uranium contamination in both groundwater and soils. Also, past weapons manufacturing operations have discharged large amounts of uranium to the subsurface. Therefore, uranium contamination is a major problem in many nuclear power plants, and US Department of Energy sites including Hanford (Washington), Savannah River (South Carolina), and Rocky Flats (Colorado).

Remediation of uranium contaminated sites has been a challenge for many years and several researchers have explored the use of different types of adsorbents for treating

uranium plumes. Uranium is not only toxic but is also radioactive. In the natural environment, uranium primarily exists in the form of hexavalent ion U(VI). Even at trace concentration levels, the toxic nature of uranium can pose major health problems. Due to its chemical and radiological toxicity, migration of uranium from the contaminated sites poses considerable health and environmental hazard (McDiarmid, 2001). The US Environmental Protection Agency (USEPA) standard for uranium concentration in drinking water is 30 μg/L (USEPA, 2004).

The local background radiochemical and radiometric settings that determine the cleanup standards for uranium are often poorly known. The National Uranium Resource Evaluation program of the Department of Energy completed a national airborne radiometric and aeromagnetic reconnaissance survey that gathered gamma-ray data from almost all of the U.S. and Alaska. Background uranium levels were obtained and the data is shown in Figure 1. The data indicates that the uranium contamination is very high in the western parts of Arizona, New Mexico and Nevada, and also in the eastern parts of Ohio. Palo Verde, the largest nuclear power plant in the US, is present in the State of Arizona. Perry and Davis-Besse are the two nuclear power plants that are present in Ohio. The wastes from these plants could be the main cause of high uranium levels in these regions. Though there are many nuclear power plants in Minnesota, Washington, Florida and Oregon the uranium levels are low in these states. This is perhaps due to effective disposal of waste management strategies practiced by these plants (EIA, Energy Information Administration).

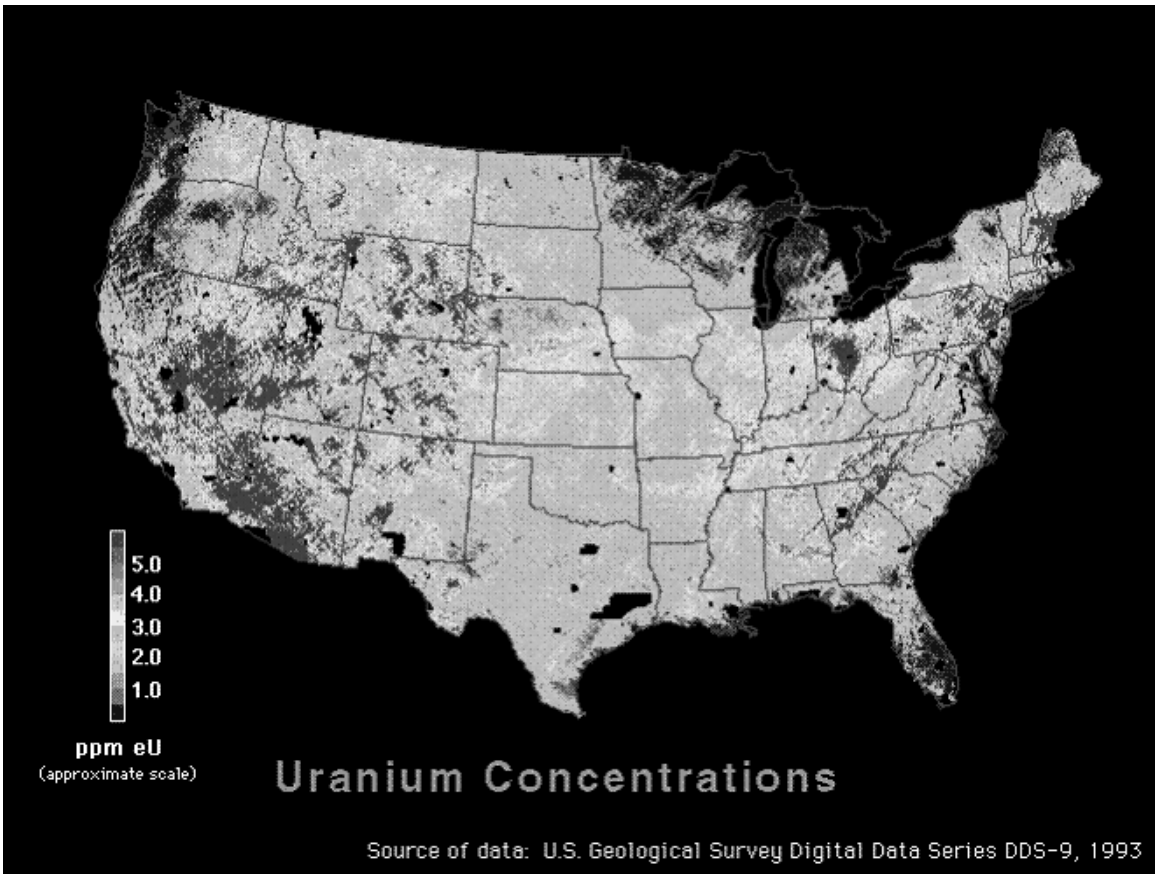

Figure 1: Uranium concentration across USA in rocks and surface soils. (Source: USGS)

Both chemical and radiological toxicity result from uranium exposure. Kidney toxicity is the main health effect associated with uranium exposure. Breathing air containing uranium dusts or consuming substances containing uranium can result in kidney toxicity. The uranium compounds enter via blood stream and are filtered by the kidneys; the filtered uranium can damage kidney cells. Acute kidney failure and death are the results of high uranium intakes (ranging from about 50 to 150 mg, depending on the

individual). Alpha particles emitted by various uranium isotopes can cause radiological toxicity. Workers in the vicinity of large uranium storage facilities can be exposed to the radiation emitted by uranium decay products. The increased probability for cancer is the primary health effect of radiological toxicity. Radiation exposure may cause cancer years after the exposure, and in some cases, it may be indistinguishable from other "naturally occurring" cancers. Some of the general illnesses caused by uranium particles are acute immunity depression, acute respiratory failure, glandular carcinoma, chronic kidney, and liver disorders. Children exposed to uranium can suffer from dyspraxia and malformations of legs, arms, toes and fingers (Akira Tashiro, Discounted Casualties: The Human Cost of Depleted Uranium).

The risks posed by uranium contaminated groundwater aquifers raise serious public health concerns and hence the site managers and regulators are interested in remediating uranium-contaminated aquifers (Han et al., 2007). Use of permeable reactive barriers (PRB) is one of the common technologies used for remediating uranium plumes (Fuller et al., 2003). Several types of sorbent materials have been used within a PRB to remediate uranium plumes. These materials include reactive sorption media such as activated carbon, zero-valent iron (ZVI), zeolites, phosphate rocks, and hydroxyapatites (Phillips et al., 2008; Han et al., 2007). Among these alternatives, hydroxyapatite (HA) has received considerable attention in recent years for removing heavy metals (Thakur et al., 2005). This is because, HA can react with heavy metals and to form minerals that are stable across a wide range of geological conditions (Nriagu, 1974; Conca and Wright 2006). For example, the solubility product of unreacted apatite

is $K_{sp} = 10^{-20}$ (Conca and Wright 2006) and that of uranium-apatite minerals, autunite $K_{sp} = 10^{-49}$ (Raicevic et al., 2006) and chernikovite, around $10^{-45.48}$ (Grenthe, 1992). It has been observed that sedimentary and/or biogenic apatites deposited by seawater can sequester metals and radionuclides into their apatite structure for many years. The sequestered metals also have little or no possibility for desorption, leaching or exchange, even under extreme diagenetic conditions that can severely change pore-water chemistry, pH, temperatures variations (of more than 500 °C), and/or result in tectonic disruptions (Skinner, 1989). Under laboratory conditions, various forms of apatites have been used for removing different types of heavy metals including Pb, Pu, Cd, Zn, Co, Cs, Th, As, Se, Cs, and Sr, Cr, Mn, Cu, U, and Ni (Del Rio et al., 2006; Conca and Wright, 2006).

The affinity of apatite for uranium has been studied extensively by Arey et al. (1999) and Krestou et al. (2004). The mechanism of uranium interactions with hydroxyapatite (HA), and their implication for groundwater remediation in batch studies have been investigated by Fuller et al. (2002). HA can complex with uranium to form stable minerals such as chernikovite ($((H_3O)_2(UO_2)_2(PO_4)_2 \cdot 6(H_2O))$ and autunite ($Ca(UO_2)_2(PO_4)_2.10H_2O$) (Fuller et al., 2002).

There are two types of apatites available--- natural apatites and synthetic apatites. Natural apatites are the ones prepared from animal bones and produced from phosphate-rich rocks. Synthetic apatite is prepared by chemically reacting a hydroxide source (calcium hydroxide) with a phosphate source (phosphoric acid).

Material extracted from fish bones is an important source of natural hydroxyapatite due to the fact that there is a large amount of fish wastes being generated daily by fish processing companies. This has the unique advantage of recycling a waste product for treating uranium. Though several studies have been completed to investigate the use commercial hydroxyapatite for treating metal wastes, only a few studies have focused on characterizing the interaction of apatite derived from fish bone with uranium. It has been fairly well established that commercial hydroxyapatite has a very high capacity for sorbing uranium; however, the cost could be prohibitive. On the other hand, since fish bone apatites can be prepared from fish wastes it can be an inexpensive alternative sorbent.

1.2 Objectives

Our preliminary review indicated that HA derived from fish bones is an excellent sorbent that has the potential for treating various types of dissolved metal plumes including uranium. Fish bone HA can be produced inexpensively by recycling the waste materials generated from fish processing plants. Catfish farming is one of major agricultural industry in the South-Eastern regions of the US and reusing the wastes from this industry offers both economic and environmental benefits. The goal of this research is to study the feasibility of using HA derived from catfish bones to remove uranium from contaminated groundwater. The specific objectives are to: (i) prepare and characterize the HA materials derived from catfish bones (CFHA), (ii) conduct batch

experiments to study the influence of various physio-chemical conditions on CFHA and U(VI) reactions, and (iii) conduct column experiments to investigate the U(VI) efficiency in PRBs containing CFHA.

1.3 Organization of Thesis

This thesis is organized into four chapters. Chapter 1, the current chapter, provides a brief introduction to uranium contamination and also reviews different types of apatites that can be used for uranium remediation. In Chapter 2, a thorough literature review is presented to document the published information regarding the removal of heavy metals by various types of hydroxyapatites. Chapter 3, which uses a journal format, provides the preparation procedure for deriving natural apatite from catfish bones, materials and methodology used in the laboratory work, details of our batch and column experiments, and a comprehensive analysis of the experimental results. Chapter 4 presents the summary and conclusions along with a discussion of potential ideas for research future work that could be done in this area.

CHAPTER 2

LITERATURE REVIEW

Hydroxyapatite (HAP) is a phosphate crystal of calcium which has a replaceable hydroxyl ion. The empirical formula of HAP is $Ca_5(PO_4)_3(OH)$. The OH^- ion in the crystal may be replaced by metals, halides or carbonates. Most natural bone material contains about 70% of hydroxyapatite (Wikipedia). Therefore, bones and teeth are very good sources of hydroxyapatite (Thomson et al., 2003). HAP interacts very well with lanthanides and actinides (Jerden and Sinha, 2003). Actinides form surface complexes, and rare earth elements substitute calcium in the crystal lattice of HAP (Jones et al., 1996). The sorbed metals react and form stable metal-phosphate minerals with apatites. Uranyl phosphate mineral, which is formed when uranium interacts with HAP, is so stable that temperatures as high as 800-1200°C may be required to decompose the mineral. Stability under a wide range of geological conditions is a very attractive property of apatites (Nriagu, 1974). The metals adsorbed by apatite cannot be desorbed, leached or even exchanged, at a broad range of pH and temperature (Conca and Wright, 2006).

2.1 Mechanism of metal sequestration within apatites

Apatites have been used for removing various types of heavy metals including Pb (Ma et al., 1993; Conca and Wright, 2006; Hettiarachchi and Pierzynski, 2004), Pu (Moore et al., 2005), Cd (Gomez del Rio et al., 2006; Conca and Wright, 2006), Zn (Gomez del Rio et al. 2006; Conca and Wright 2006), Co (Gomez del Rio et al., 2006), Cs (Seaman et al., 2001), Th (Ulusoy and Akkaya 2008), As, Se, Cs, and Sr (Thomson et al., 2003), Cr (Ozawa et al., 2003), Mn (Ozawa et al., 2003), Cu and U (Wright et al., 2004), and Ni (Seaman et al., 2001).

Apatite form phosphate compounds, with very low solubility, after reacting with the metals such as Pb, U, Cd, Zn, Cu and Al. The low solubility product ($K^{sp} = 10^{-20}$) of apatite and the metal phosphate is the reason for their high stability. Under field conditions, the main factors that influence the sorption reaction of apatites within a permeable reactive barrier (PRB) are the grain size, flow rate and barrier thickness. The phosphates, Cr^{3+} ions and fulvic acid also have effect of U(VI) sorption (Hongxia et al., 2009 a, b). Apatites can react rapidly with metals and hence, at times, it is difficult to quantify the rate of the removal process. (Koeppenkastrop and De Carlo, 1990; Ma et al., 1993; Wright et al., 1995; Chen et al., 1997).

Conca and Wright (2006) used fish bone apatite in a PRB to remediate zinc, lead and cadmium contaminated groundwater. They reported four types of processes that facilitate apatite reaction with heavy metals. First, HA can continuously supply a small amount of PO_4^{-3} to solution to exceed the solubility limits of various metal phosphate

solids; this helps precipitate metals based upon the metal concentration and solution conditions. Secondly, the apatite dissolution process can buffer solutions at an increased pH level, this can help precipitate many metal-bearing phases. Thirdly, HA can adsorb metals directly to its surface through chemi- adsorption. Finally, bone apatites promote biological activities and this could lead to certain biochemical conditions that favor metal precipitation. For example, at the success site, Zn sequestration on an apatite barrier was facilitated by the biological stimulation of SO_4^{2-} reducing bacteria, followed by the precipitation of ZnS (Conca and Wright, 2006).

Dissolution of HAP can yield free phosphate ions in solution. The kinetics of the HAP dissolution process has been investigated in detail by Tang et al. (2004). The dissolution process starts by causing a pit and the pit can spread in the form of stepwaves. Large pits contribute to the spreading of the stepwaves. The dissolution kinetics of nanoscale HAP crystals can be explained using rate law by accounting for the crystal size (Tang et al., 2004).

Krestou et al. (2004) studied uranium interactions with HA and reported that about 95% of uranium removal occurs within a short time via bulk precipitation. They found that depending on the experimental pH, the precipitated uranium complex can form either $Ca(UO_2)(PO_4)_2$ or $CaUO_2(CO_3)_2$. The mechanism of sequestration of uranium by hydroxyapatite in particular was studied in detail by Fuller et al. (2002). Using X-ray diffraction (XRD) and X-ray absorption spectroscopy (XAS) methods they observed that phosphates, carbonates or hydroxides of uranium could not be formed at lower uranium concentrations (<4700 ppm), suggesting that the removal takes place primarily through

surface adsorption of uranium on HAP as an inner-sphere complex. At higher concentrations (>7000ppm), the formations of chernikovite[$(H_3O)_2(UO_2)_2(PO_4)_2 \cdot 6(H_2O)$] and autunite [$Ca(UO_2)_2(PO_4)_2.10H_2O$] were observed. Hence, the authors concluded that uranium removal by HAP is governed by a surface complexation mechanism at lower concentrations and uranyl phosphate precipitation at higher concentrations. The transition from complexation mechanism to precipitation mechanism takes place at around 5800±800 ppm uranium concentration, after which chernikovite will be formed. Fuller's research team later used commercial HA within a PRB to treat an uranium plume in a shallow alluvial aquifer at Fry Canyon, Utah (Fuller et al., 2002; SSRL, 2003).

The mechanism of uranium removal by apatite occurs through one of the following three types of reaction. The first mechanism is ion-exchange, in which the uranyl ions replace the divalent calcium ions from the apatite structure thus removing uranium from the liquid phase.

$$\equiv Ca^{2+} + UO_2^{2+} = \equiv UO_2^{2+} + Ca^{2+}$$

Surface complexation is the second mechanism in which uranium removal occurs by attachment of the uranyl ions to the phosphate or hydroxyl ions as shown below.

$$\equiv OH + UO_2^{2+} = \equiv O\text{-}UO_2^{+} + H^{+}$$

$$\equiv O_3P\text{-}OH^{+} + UO_2^{2+} = \equiv O_3P\text{-}O\text{-}UO_2^{2+} + H^{+}$$

Third mechanism is precipitation, which occurs via dissolution/precipitation reaction with phosphate ions and subsequent formation of two stable metal phosphates, namely, autunite and chernikovite (Simon et al., 2008).

$$Ca_5(PO_4)_3(OH) = 5Ca^{2+} + 3PO_4^{3-} + OH^-$$

$$2H^+ + 2UO_2^{2+} + 2PO_4^{3-} + nH2O = H_2[(UO_2)(PO_4)]_2X\ n\ H_2O$$

(chernikovite)

$$Ca^{2+} + 2UO_2^{2+} + 2PO_4^{3-} + nH_2O = Ca[(UO_2)(PO_4)]_2X\ n\ H_2O$$

(autunite)

The mechanism of the autunite formation has been studied in detail by Ohnuki et al. (2004).

2.2 Apatite from natural sources

Preparation of apatite from natural sources, such as animal bones, has been studied by many researchers. Hwang et al. (2006) did experiments with waste bones of cows, pigs and tunas. Biltz and Pellegrino (1969) completed a detailed comparison study of the chemical composition of bones of sixteen vertebrates which included cats, monkeys, fishes, turtles, frogs, humans, elephants, polar bears, horses, to name a few. Their data indicate that the percentage of phosphate and apatite is relatively high in fish bones. Conca and Wright (2006) used a mixture of fish bones to prepare apatite and found it has a general composition of $Ca_{10-x}Na_x(PO_4)_{6-x}(CO_3)_x(OH)_2$ where $x<1$.

Fish bone apatite is produced after processing the fish wastes from the industries through a series of steps. The fish bones can be either mechanically-, enzymatically-, or thermally-treated before using them as an absorbent in the batch and column experiments. Martin et al. (2008) observed that with aging, the mechanically and enzymatically treated fish bone apatite produced higher dissolved organic carbon (DOC) and biochemical oxygen demand (BOD) concentrations than those produced by thermal treatments. In the above study, mechanical treatment was done by removing most of the flesh and organic portions of the fish by cutting, pressing, steaming and hot-air drying. Enzymatic treatment was done by using an enzymatic digestion process that removed all bioavailable organics (Slater, UK; Martin et al., 2008). Thermal treatment was done by placing approximately 1 kg of unaltered mechanically treated apatite into a muffle furnace and heating it at a high temperature for 24 hours.

2.3 Fish Bone Ceramic

Large number of micropores and macropores form the structure of Fish bone. When a sample of fish bone is heated at 800°C the grain size is around 200 nm and when heated at 1000°C the grain size is around ~500 nm. Thus, thermal treatment results in increasing the grain size. In both the cases the grains were prolonged spherical particles. After heat treatment at high temperatures (600°–1300°C), the medium porosity is lost and the walls of fish bones form a dense body. The resultant bone-originated ceramic has a dense, sintered shell form, a replica of the natural macroporous structure of fish bones.

Microstructural developments occur when fish-bone apatite is heated at high temperatures. This fish bone ceramic is an inexpensive ceramic media and is a biologically and environmentally compatible material (Ozawa and Suzuki, 2002)

The transition of apatite upon heat treatment is well-explained by Ozawa and Suzuki (2002). When heated at temperatures between 800°–1200°C the bones transition to form a well-crystallized hydroxyapatite crystal, which then changes to HAP ceramic with tricalcium phosphate (TCP) phase at 1300°C. The phase transformation of synthetic hydroxyapatite to TCP occurs at ~1250°C and his information is consistent with the studies done by Yamashita and Kanazawa (1989). Thus, by heating fish bone at temperature < 1200°C HAP ceramics is produced and by further increasing the temperature to 1300°C a sintered composite of TCP/hydroxyapatite can be produced (Ozawa and Suzuki, 2002).

2.4 Effect of Organics

Both the organic content of the solution and the organics present on the fish bone apatites can affect the uranium sorption process. Arey et al. (1998), who studied the effects of organic content of the solution on uranium removal, reported that low pH values observed in organics rich sediments is responsible for maintaining a higher liquid-phase uranium concentration. Another reason for high aqueous phase uranium concentration in organic rich environment is that the solubility of metal can be increased by complexation with the dissolved organic carbon (DOC) (Arey et al., 1998).

Martin et al. (2008) investigated the effects of residual organic matter present on the fish bone and its influence on metal removal properties. Three types of fish bone apatites were prepared using mechanical, thermal and enzymatic digestion processes to test their efficiencies for removing lead were studied. The results indicated that the organics associated with fish-bone based apatite can inhibit metal removal from the solution phase via two mechanisms: 1) by stimulating biological growth on the surface, which can impede surface adsorption; and 2) decreasing phosphate ion concentration in the solution by consuming it as a nutrient source for supporting the biological activity. It was also observed that the thermally treated (baked) apatite removed Pb rapidly from the solution when compared to mechanically-treated and enzymatically-digested apatites.

2.5 HAP and Fish bone apatite as PRB

Permeable reactive barrier (PRB) is a reactive barrier that is installed under the ground to treat contaminant plumes (NAVFAC, US Navy website). The use of fish bone apatite as a PRB material to remove various metals has been reported by Conca and Wright (2006). Conca and Wright set up a PRB to remove Zn, Pb, Cd, Cu, SO_4, and NO_3 and its performance was observed for 4 years. About 4550 kg of Zn, 91 kg of Pb and 45 kg of Cd were removed by 90 tonnes of apatite. The metal loading capacity was far higher compared to other usually used adsorbents such as phosphate rock, cow bone, C-sorb, zeolites clinoptilolite and chabazite, Fe^0 filings, compost, and activated charcoal (Conca and Wright, 2006).

Uranium removal using commercial hydroxyapatite PRB was studied by Simon et al. (2008). In the city of Pecs in Hungary a waste rock pile with 60 g/ton U was deposited over an aquifer that was used for drinking water. The aqueous uranium concentration levels increased from 200 µg/L in 1996 to 800 µg/L in 2000. Project PEREBAR was undertaken in this area to remediate the uranium contaminated groundwater using a PRB technology (Roehl et al. 2005). The study found that Ca content in the apatite and the carbonate concentrations were important factors that influenced uranium removal processes within the PRB.

2.6 Removal efficiencies

Apatite has high removal efficiencies for Pb, Cd, and Zn. The capacity of apatite for removing Pb, Cd and Zn, as reported by Chen et al. (1997), are: 151 mg Pb/g of apatite, 73 mg of Cd/g of apatite, and 41 mg of Zn/ g of apatite. Thus lead removal efficiency is the highest and it is removed by precipitation of hydroxyl fluoropyromorphite. For Zn and Cd the removal the mechanisms include ion exchange, surface complexation and precipitation reactions.

For uranium, hydroxyapatite showed high removal efficiency in the pH range between 3 and 11, which was independent of the presence of carbonates and sulfates. The removal capacity of hydroxyapatite observed by Krestou et al. (2003) was 20 mg U/g HAP. The maximum efficiency of removal occurred within the pH range of 5 to 8.5 (Krestou et al., 2003).

2.7 Factors affecting sorption on hydroxyapatite

For optimal sorption, apatite must have high internal porosity, low fluorine substitution in hydroxyl ion position, high carbonate ion substitution, sufficient sites for nucleation, and have few trace metals in their structure (Wright et al., 2004). Thakur et at (2005) showed that uranium removal efficiency would depend on the amount of sorbent, ionic strength, U(VI) concentration, pH, and temperature. The rate of uranyl ion sorption decreased with increasing ionic strength and uranyl concentrations. The maximum sorption occurred with the pH range of 7-8 (Thakur et al., 2005).

2.8 Column Experiments using hydroxyapatite

Thomson et al. (2003) conducted experiments to compare the efficiencies of various sorbents for removing dissolved metals and radionuclides. The nine adsorbents used for the study were: various types of synthetic apatites, tri-calcium-phosphate, fish bones, cow-bone char, clinoptilolite, and activated magnetite. These materials were tested for removing four radionuclies: Am, Pu, Tc and U, and two oxyanions As and Se. A simulated groundwater that replicated the composition of the groundwater present at Rocky Flats was used. Single point batch adsorption experiments were completed and bone char, commercial apatite and and tri-calcium phosphate were selected as the best sorbents. The performances of these sorbents were further tested by conducting batch isotherm and column studies near neutral pH. The results indicated that synthetic apatite

and tri-calcium phosphate have high capacity for removing both redionuclides and oxyanoins.

Mibus and Brendler (2006) completed column experiments to study U(VI) sorption by HA. They used synthetic groundwater which was similar to one present at a uranium mining site in Schlema, Germany. Geochemical modeling indicated that a neutral uranium complex, $Ca_2UO_2(CO_3)_3$ is expected to be the predominant species at their solution pH value of 7.83. The Fluorescence spectra confirmed that this was indeed the dominant species. The column results indicated a retardation factor varies in the range of 27 to 45, for soils containing 0.1% of pure HA at a solution pH of 7.83.

2.9 Fish bone as a substitute for hydroxyapatite

Natural apatite from fish bone can be used as a substitute for HAP for remediating aqueous heavy metals (Admassu and Breese, 1999). They found that fish bone apatite has the capacity to remove various metals and radionuclides including Pb^{2+}, Cu^{2+}, Cd^{2+} and Ni^{2+} to below detectable levels. Chromium removal by fish bone apatite from groundwater has been studied by Ozawa et al. (2003). Pb removal by fish apatite has been investigated by Ozawa and Kanahara (2005). Wright et al. (2004) found that using fish bone apatites the remediation cost was $40 per 1,000,000 gallons of water per mg/L of metal, and for soils it was \$20-\$30 / yd^3. Thus, fish bone can serve as a cost-effective substitute for HAP for use in PRBs employed for treating metal plumes.

CHAPTER 3

USE OF HYDROXYAPATITES DERIVED FROM CATFISH BONES FOR REMEDIATING URANIUM CONTAMINATED GROUNDWATER

This chapter provides a comprehensive summary of the all the experimental work completed in this study. The information is organized into three major sections including materials and methods, experimental design, and results and discussions. The format is similar to the one used by Science of Total Environment, Elsevier environmental science journal.

3.1 Material and Methods

All the chemicals used in the experiments were reagent grade. Several chemicals including sodium nitrate and sodium bicarbonate, sodium hydroxide and nitric acid were purchased from Fisher (Fisher Scientific, Fairlawn, NJ, USA). Commercial hydroxyapatite was purchased from Aldrich (Sigma-Aldrich, St. Louis, MO). The acids were trace-metal grade. The uranium solution was prepared from plasma-grade uranium-standard made using depleted uranium.

Catfish waste products were collected from a catfish processing plant. The waste was boiled for about two hours. The cooked waste was washed in a flowing stream of water

to remove bulk flesh and fat materials (See Appendix-I for detailed photographs). The remaining material was then soaked in 30% hydrogen peroxide for a day to remove all residual organic matter. The treated bones were air dried for two days and then crushed into smaller pieces and heated in an oven for three days. In order to investigate the effects of heat treatment, two types of sorbents were prepared by heating the bones at 100 °C and 300 °C. Furthermore, in order to study the size effects, the fish bones prepared at 100 °C were mechanically crushed and sieved to yield material with large(>2000 µm), medium (300-2000 µm) and small (< 300 µm) particle sizes.

3.2 Design of the batch experiment

Batch adsorption experiments were conducted at room temperature (~295 K) in 50-mL polycarbonate centrifuge tubes with each tube yielding one data point. All of the experiments were completed in duplicate. The samples were prepared by adding an appropriate amount of the hydroxyapatite, ionic strength adjuster (0.01M $NaNO_3$), $NaHCO_3$ (0.01M), acidified U(VI) stock solution [$UO_2(NO_3)_2$], and deionized water. Babu et al. (2008) reported that uranium concentration in groundwater ranged from 0.3 to 1442.9 µg/L. In our study, we used concentrations around 1 ppm in both batch and column experiments. In all the batch experiments, the pH of the solution was adjusted (set at either pH 7 or 8.5) using 1 M NaOH or HNO_3. The equilibrium aqueous U(VI) concentrations in the adsorption kinetic experiments and the adsorption isotherm experiments were 2.4×10^{-6} M, which is within the ranges used by other researchers to

represent typical U(VI) concentrations in contaminated groundwater (Cheng et al., 2006). The vials were capped quickly (to minimize CO_2 exchange) and were shaken for about 72 hours (this time was adequate to reach equilibrium and was determined based on kinetic data shown below). The pH values were recorded before and after the reaction. The reacted samples were opened, and an aliquot of the supernatant was withdrawn and immediately filtered with a 0.45-µm syringe filter. The filtrate was used to measure the aqueous U(VI) concentrations.

The U(VI) concentration was analyzed using a kinetic phosphorescence analyzer (KPA-11, Chemchek Instruments, Richland, WA). The filtered samples were acidified to lower the pH value close to 1.5. The uncertainty in detection limit of the U(VI) analysis was ±3% (Cheng et al., 2004). The total calcium concentration was analyzed using a flame atomic absorption spectrophotometer (AAS 220FS, Varian, Palo Alto, CA).

3.3 Design of the column experiment

One dimensional columns with 1 cm diameter and 10 cm length were used in our experiments. About 1.5 gm of fish bone and 7.5 gm of ottawa sand (unless otherwise mentioned) were mixed thoroughly and dry packed into the column. The column was tapped at regular intervals to ensure uniform packing. The column setup is shown in Figure 2. As shown in the picture, the column was run in a vertical mode and the feed solution was injected into the bottom of the column and the effluent was sampled from the top, either manually or using a fraction collector. A large amount of uranium feed

solution, with a known U(IV) concentration, was prepared. Sufficient ionic strength adjuster and buffer solutions were added. The final pH was adjusted to the desired value and the solution was pumped at different rates into the column using an HPLC pump. Some glass wool was placed at the end of the column to prevent washout of the solid material. When manual sampling was employed, the uranium solution from the outlet was collected at regular time intervals in 50-mL polycarbonate centrifuge tubes. After each experiment, the column was emptied, cleaned with concentrated HNO_3 and water. The experiments were repeated at least twice to verify reproducibility.

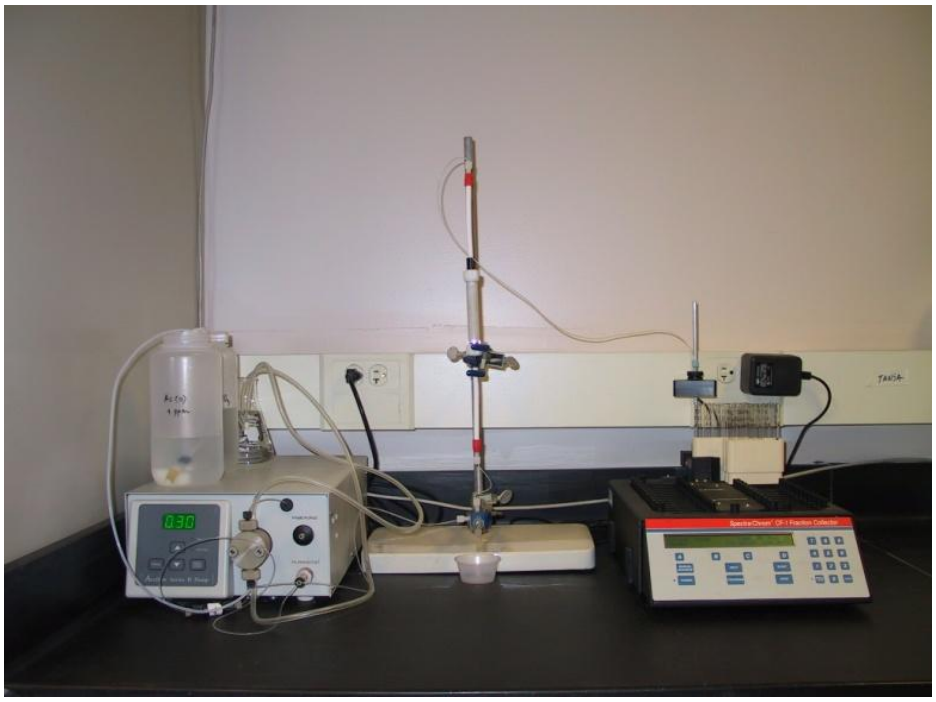

Figure 2: Typical column setup used in this study

3.4 Results and Discussion

Solid phase characterizations of catfish hydroxyapatite (CFHA)

Samples CFHA were also prepared by dropping a small amount of CNT solution on a mica substrate and air-drying it overnight. These samples were then coated with a thin layer of gold (~10 nm) and imaged using a JEOL JSM 7000F field emission scanning electron microscope equipped with an energy dispersive X-ray analyzer (JEOL USA). Figure 3 shows the SEM images of CFHA and commercial HA (CHA). The data shows that CHA is about 100 nm, whereas CFHA was about 50 nm.

Scanning electron microscope images

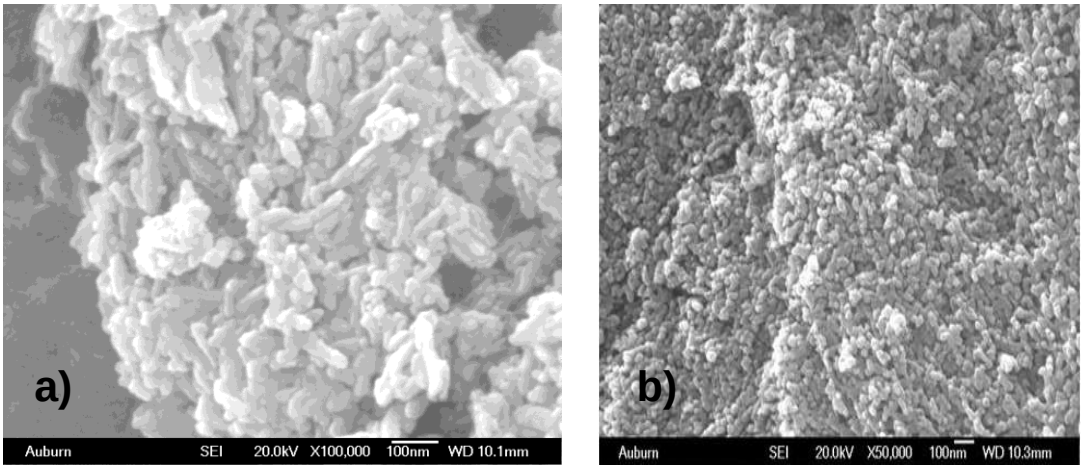

Figure 3: SEM image of a) commercial hydroxyapatite and b) fish bones

X-ray diffraction (XRD) data were collected using a Rigaku Miniflex diffractometer using Cu Kα radiation, and the data are presented in Figure 4. The data show that the XRD pattern of CFHA matches (the figure on the top) well with the XRD

pattern of CHA (bottom figure), confirming that the material derived from catfish bones was indeed HA.

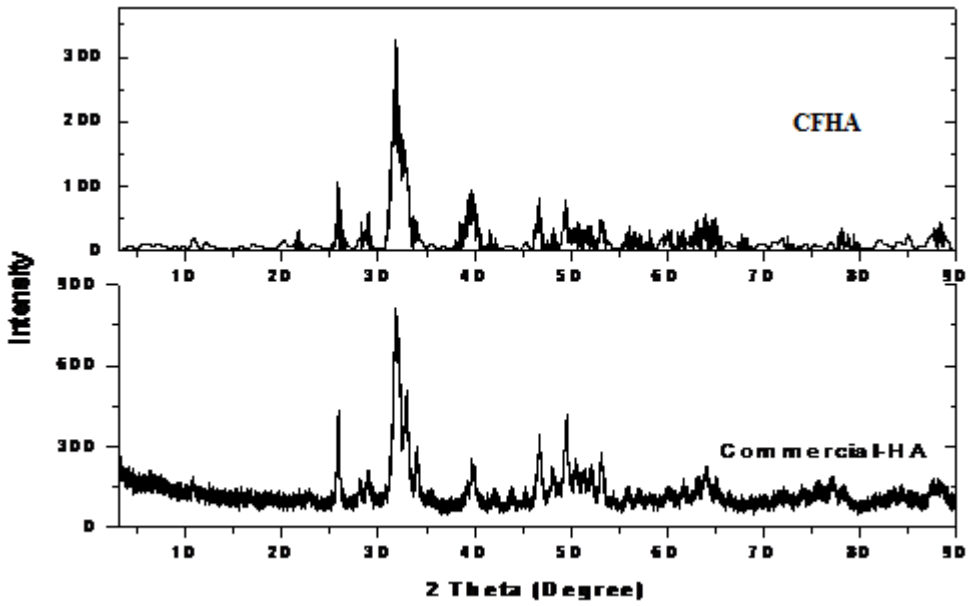

Figure 4: Comparison of XRD data of catfish bones and commercial hydroxapatite

3.5 Effect of pH

The effect of pH on U(VI) adsorption onto HA and CFHA are presented in Figure 5. The details of the experimental conditions used in these experiments are summarized in the figure caption. For commercial HA, the extent of uranium removal was 0.23-2.2 mg/g in the pH range 3-5 and decreased sharply at pH below 4 and above 9. A similar trend was observed for CFHA. The pH-dependent behavior can be explained by pH-dependent speciation and charges of both the uranium and HA. The pH dependent

sorption effect is due to the ionization of both the adsorbate and the adsorbent causing repulsion at the surface and decreasing the net U(VI) adsorption. The zeta-potential/ point of zero charge of HA is negative for pH values higher than 7.7(Krestou et al., 2004). This point of zero charge will be shifted to 7.13 when the solution is in equilibrium with atmospheric carbon dioxide (Wu et al., 1991). Below pH 7.7, HA remains positively charged and it will be negatively charged above pH 7.7. When the pH is above 7.13, HA surface becomes negatively charged, and, as the solution pH increases, uranium species also becomes negatively charged [$UO_2(CO_3)_2^{2-}$] by equilibrating with atmospheric CO_2 , which is there in vial as head space (Krestou et al., 2004). When the pH is above 9, UO_2 $(CO_3)^-$ is the predominant U(VI) species and since the iso-electric point of HA is near the pH value of 7.7, the HA product surfaces are also negative (Korte and Fernando 1991) causing electrostatic repulsion. Between 3.5 and 5.5 pH uranium exist in the form of uranyl ion which are repelled by the positive surface charge of HA. Between pH 5.5 to 7 the uranyl ion is replaced by positive or neutral uranium mononuclear and polynuclear hydroxo-complexes ($(UO_2)_3(OH)_5^+$, $UO_2(OH)_2^0$. The negative sites on HAP attract the positive charged uranium species. Therefore speciation can greatly impact uranium sorption.

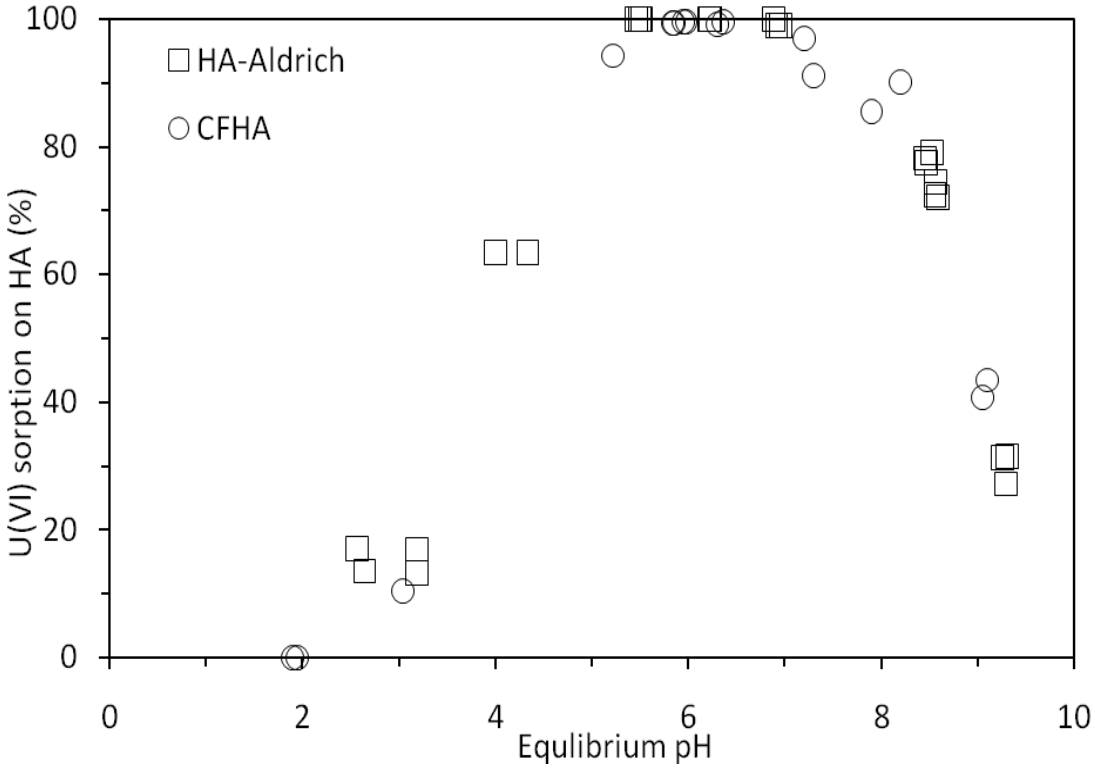

Figure 5: Influence of pH on sorption of U(VI) onto commercial hydroxyapatite and fish bones (Experimental conditions: 1mg/L of initial U(VI), 0.5 g/L of HA, 0.01 M $NaNO_3$, 0.01 M $NaHCO_3$, and pH ~2-10 at ~295K)

3.6 Effect of preparation temperature on uranium removal kinetics

The temperature used for preparing the fish bone apatite can affect its sorption properties since the surface area of the solids is influenced by the heating process . In this study, the fish bone apatite was prepared by heating the bones at 100 °C and 300 °C for

24 hours. Figure 6 shows samples of the two preparations. The particles sizes of the materials shown in the figure are less than 300 µm.

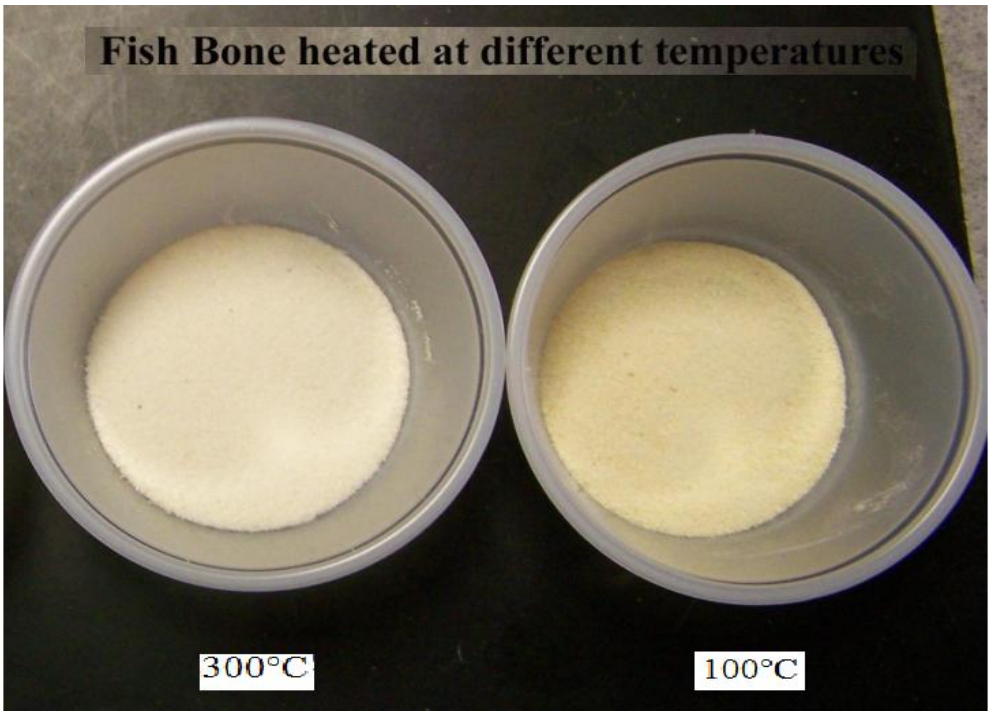

Figure 6: Images of fish bone heated at two different temperatures

Kinetics of the uranium removal process was studied using both the CFHA samples and the results are summarized in Figure 7. All the experiments were completed in duplicate using 50 ml centrifuge air tight vials at the pH value of 7. The results show that the preparation (temperature at which cat fish bone apatite were dried in the oven) influenced the removal kinetics. Ozawa and Suzuku (2002) used three preparation temperatures of 600°C, 800°C and 1000°C on fish bones and found that the surface area of the particles decreased with increases in the oven temperature.

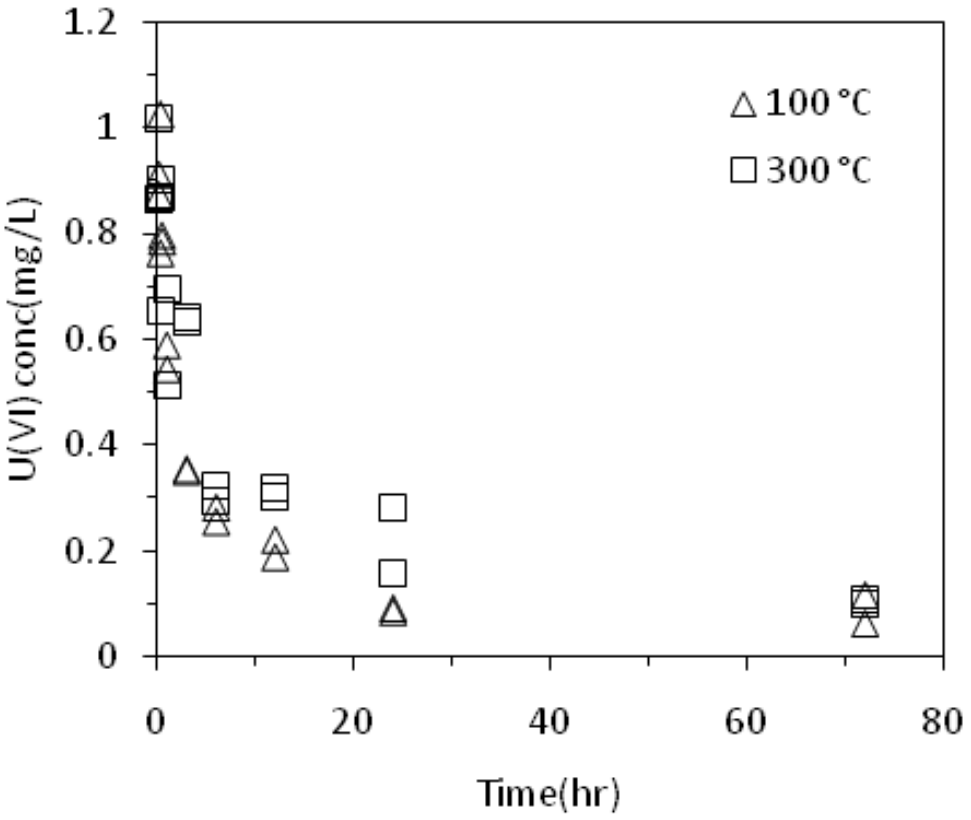

Figure 7: Effects of CFHA preparation temperature on the kinetics of uranium removal process (Experimental conditions: 1 mg/L of initial U(VI), 0.5 g/L of CFHA, 0.01 M $NaNO_3$, 0.01 M $NaHCO_3$, pH 7 and room temperature)

The preparation temperature of 600°C yield apatites with the maximum surface area of 10.5 m^2/g, while 800°C and 1000°C had surface areas of 4 and 1.6 m^2/g, respectively. Ozawa et al. (2003) showed that preparation temperature of 600°C is more effective than 900°C for removing Cr. Our results in Figure A1-1 show a similar trend.

The thermal effect leads to decrease in the surface area of the particles and hence the U(VI) removal capacity has been found to decrease with increase with temperature. From the microscopic images we can conclude that, the lower the preparation

temperature, the higher is its specific surface area and hence, higher is its adsorption capacity (though not significant). Therefore, from now on CFHA prepared at 100 °C will be used for all the experiments.

3.7 Effect of Particle size of catfish bone on uranium removal

The CFHA material prepared at 100 °C was crushed in a blender to prepare sample with different particle sizes. Particles of three different sizes (> 2000 µ, between 2000 µ and 300 µ, and < 300 µ) were obtained by sieving the crushed samples. A digital picture of these samples is shown in Figure 8a.

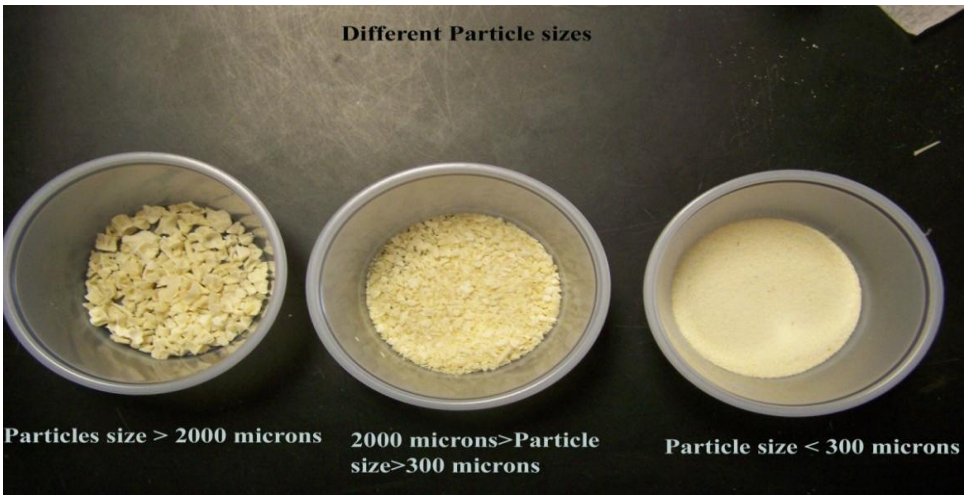

Figure 8a: Image of fish bone hydroxyapatite with different particle sizes

Surface area plays a vital role when the sequestration mechanism is adsorption. Surface area of a particle is the area exposed by the particle for adsorption. The dimensions of the particle determine its surface area. When the particle is broken into

smaller particles there is new area being created, which results in an increase in surface area. This is shown in Fig (8b).

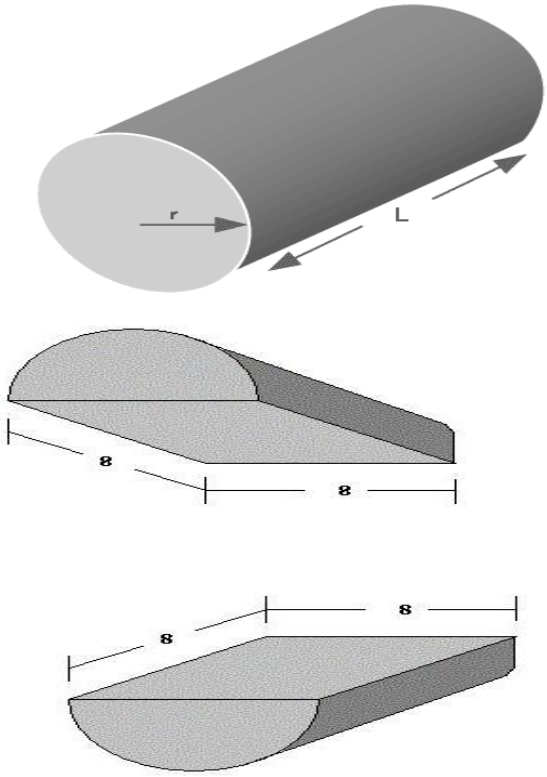

Figure 8b: Depiction of increase in surface area when the cylinder is cut into two.(Figure source: BBC, 2009)

The kinetics of the uranium removal process was studied using the CFHA material with the three different particle sizes. The results of this study are summarized in Figure 9. All the experiments were completed in duplicate using 50 ml centrifuge air tight vials at the pH value of 7. The data shown in the figure indicate those small sized particles CFHA are more efficient in removing uranium than largest sized particle CFHA. Since uranium interaction with HA occurs at the surface, surface area plays a significant role in

controlling the efficiency of this reaction. Since large particles have lower surface area they tend to have less efficiency. Therefore, CFHA with particle sizes less than 300 µ is the best choice and will be used in all subsequent experiments. A detailed comparison of the surface area, and distribution coefficients is listed in Table 1 in the appendix.

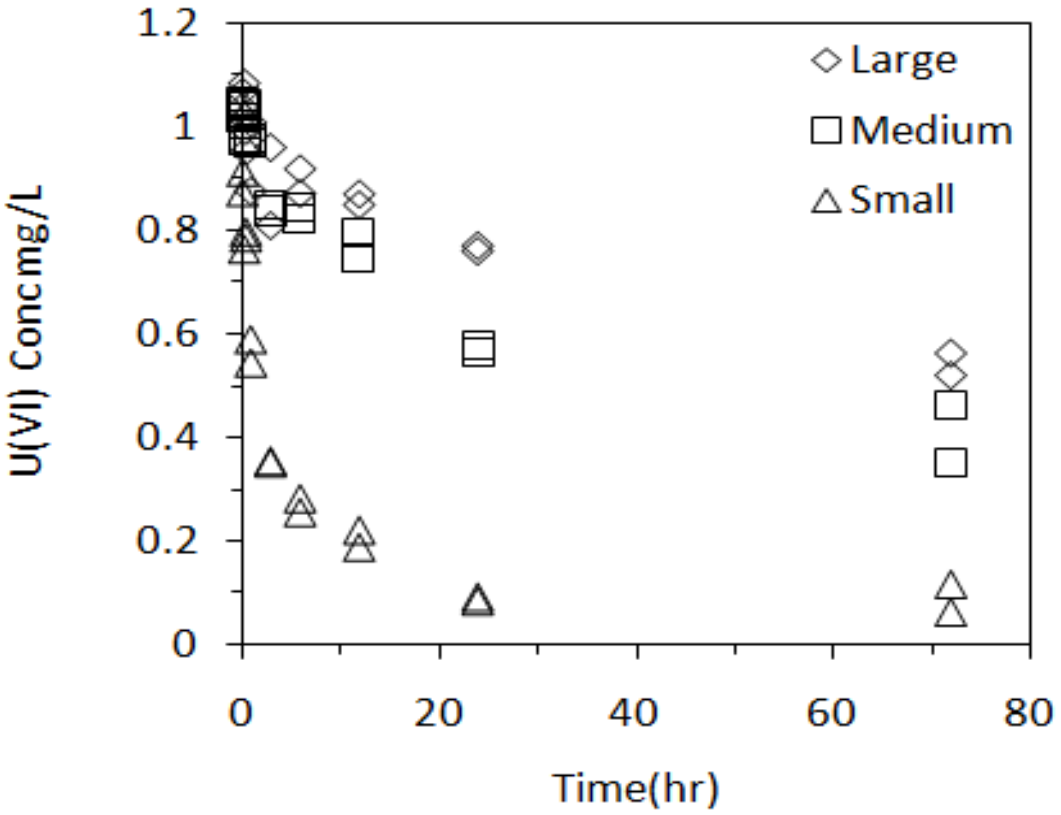

Figure 9: Effects of CFHA particle size on the kinetics of uranium removal process

(Experimental conditions: 1mg/L of initial U(VI), 0.5 g/L of CFHA, 0.01 M $NaNO_3$, 0.01 M $NaHCO_3$, pH 7 and room temperature)

3.8 Comparison of CFHA Kinetics with CHA Kinetic at different pH values

Kinetics experiments were completed to compare the removal efficiency of CFHA material with commercial hydroxyapatite (CHA) at pH values of 7 and 8.5. For comparison purposes, we also include a kinetic dataset completed at pH 8.5 using commercial hydroxyapatite. The results of this kinetic study are summarized in Figure 10. All the experiments were completed in duplicate using 50 ml centrifuge air-tight vials. The data show that the system reached equilibrium condition well within 72 hours, therefore all subsequent batch experiments were run only for 72 hours. The results also indicate that the treatment efficiency is considerably higher at the neutral pH value. It is can be estimated that at pH 8.5 about 60% of dissolve uranium was removed, whereas at neutral pH over 95% of uranium was removed. The removal efficiency of CHA at pH 8.5 is about 80% which is slightly higher than CFHA removal efficiency at pH 8.5.

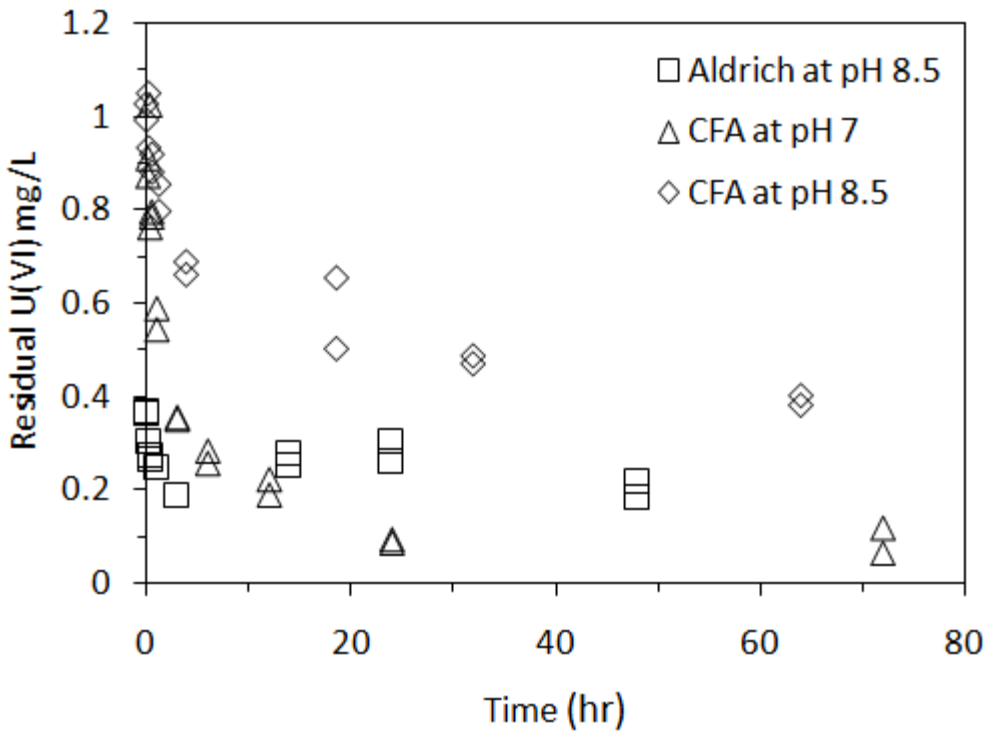

Figure 10: Comparison of uranium removal kinetics using CFHA and CHA (Experimental conditions: 1mg/L of initial U(VI), 0.5 g/L of CFHA, 0.01 M $NaNO_3$, 0.01 M $NaHCO_3$, pH 7 and 8.5, and room temperature)

3.9 U(VI) adsorption isotherms

Isotherm experiments were completed by reacting a fixed amount of CFHA (0.0250 gm) with uranium solutions with intial concentrations varying from 1 to 10 mg/L. The solid solution ratio in the batch system was 0.5 g/L, and the pH was adjusted to 7 by adding small amount of 1M HNO_3 or 1M NAOH. The batch reactors were shaken for 3 days. From the intial and final concentration measurements the amount of

uranium partioned to the solids (CFHA) were estimated and these values are plotted against the final equalibrium concentrations in Figure 11. The isotherm data shown in the figure indicates that the adsorption mechanism follows a linear trend at low liquid concentration values (until about 1 mg/L). Beyond 1 mg/L, the removal process appeared to have reached a saturation level and the data indicates that the maximum capacity (saturation level) is about 18 mg of U/ g of CFHA at the valule of pH 7.

Two additional isotherm experiments were also completed to evaluate the sensitivity of the isotherm data to pH. Figure 12 shows the isotherm data at pH 8.5 and 9. At higher pH values the isotherm is linear until an equlibrium uranium concentration value of 8 mg/L; beyond this limit the system appears to reach a saturation level. The data indicates that the maximum capacity of 12 mg of U/ g of CFHA at the pH value of 8.5 and a maximum capacity value of about 5 mg/L of U/ g of CFHA at pH 9. The results are consistent with pH edge data (Figure 5) which indicates a sharp drop in sorption between the pH values 8.5 and 9.5.

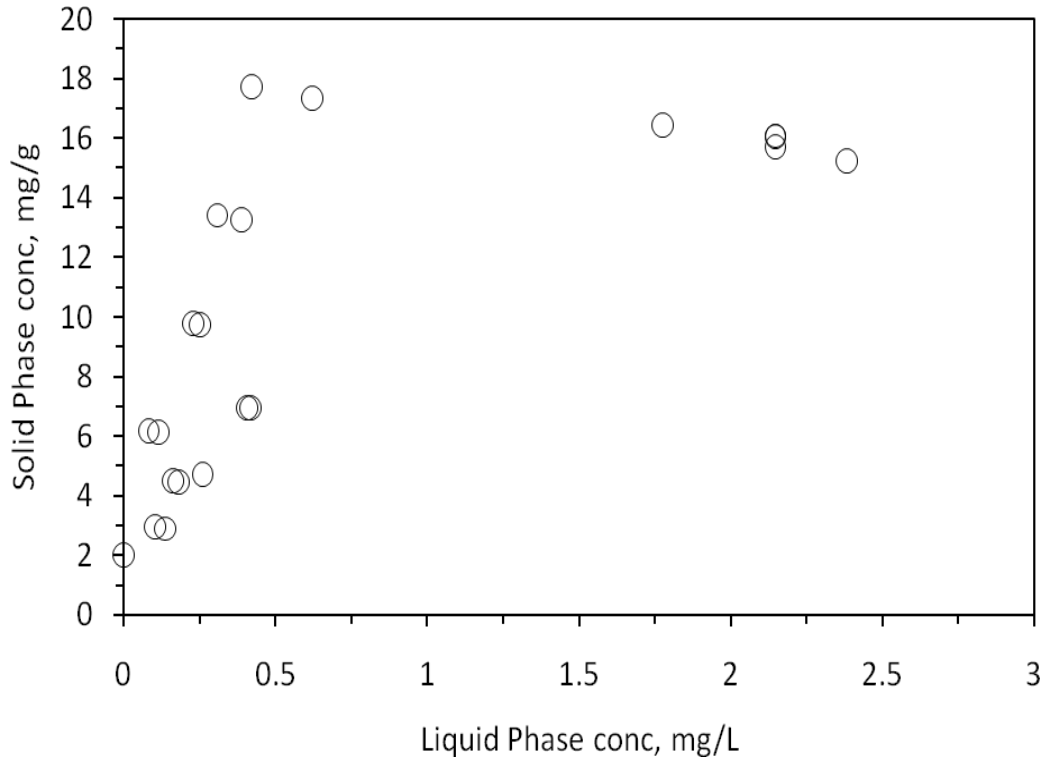

Figure 11: Isotherm data for fish bone hydroxyapatite at pH 7

(Experimental conditions: 1 to 10 mg/L of initial U(VI), 0.5 g/L of CFHA, 0.01 M $NaNO_3$, 0.01 M $NaHCO_3$, and room temperature)

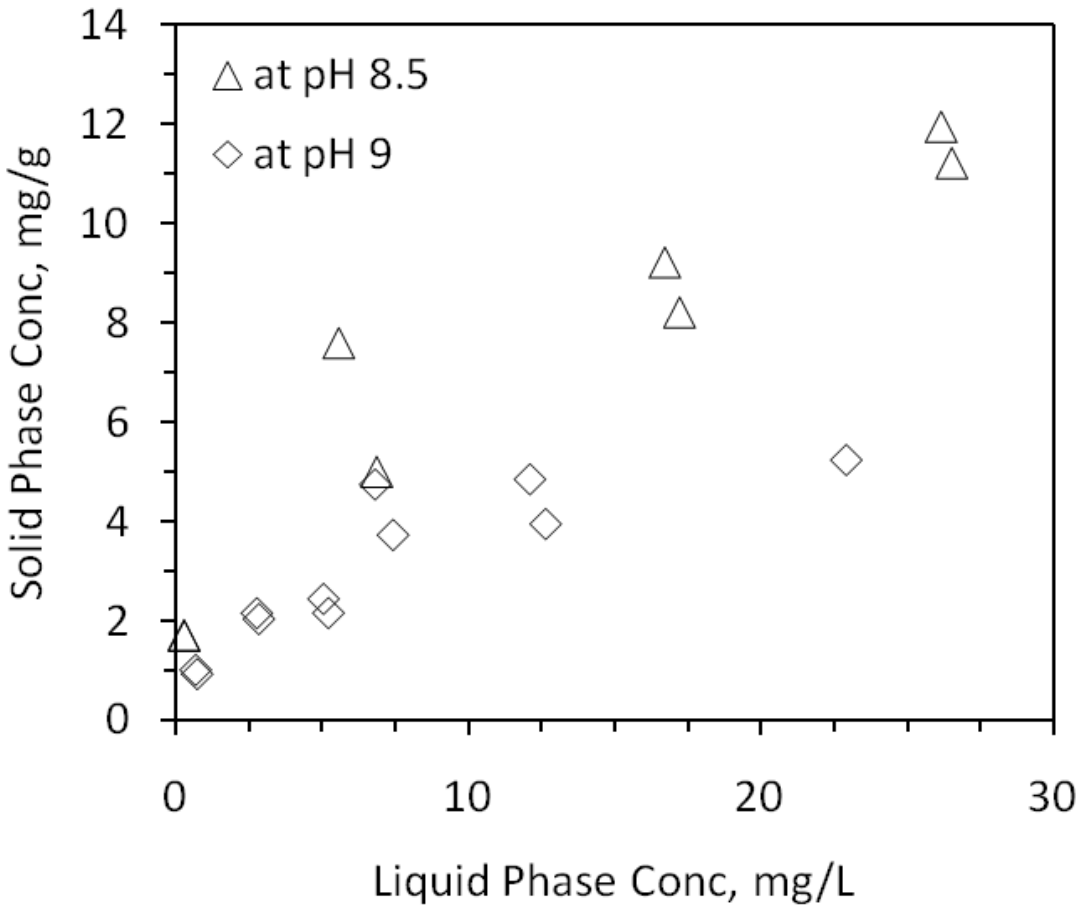

Figure 12: Isotherm data for fish bone hydroxyapatite at pH 8.5 and 9

(Experimental conditions: 1 to 30 mg/L of initial U(VI), 0.5 g/L of CFHA, 0.01 M $NaNO_3$, 0.01 M $NaHCO_3$, and room temperature)

3.10 Column experiment to study the effect of particle size on U(IV) removal

Column experiments were done to study the effects of particle size on the removal of U(VI) under flow conditions. Three column experiments were completed using the

three types of CFHA (large, medium, and small). The columns were packed with 1.5 gm of Fish bone and 7.5 gm of ottawa sand and were fed with 1 mg/L of U (VI) stock solution at a pH of 8.5. Effluents from these columns were sampled at regular intervals and liquid phase uranium concentrations and final pH values were measured. Figure 13 provides the breakthough data from the 3 columns and the breakthough from a control (sand without CFHA). The data shows that the uranium removal efficiency of the columns is a strong function of particle size. The column packed with the small CFHA particles performed better than the columns packed with medium and large CFHA particles. The breakthough occurred at around 1, 22, 880 pore volumes, respectively, for the columns packed with large, medium, and small particles. The general trend is similar to the one expected to be observed based on the batch kinetic data shown in Figure 9. The kinetic data showed that larger particles have a lower uranium removal capacity and they also have slow kinetics. The differences in the performance observed in the column experiments is due to the combination of these two effects.

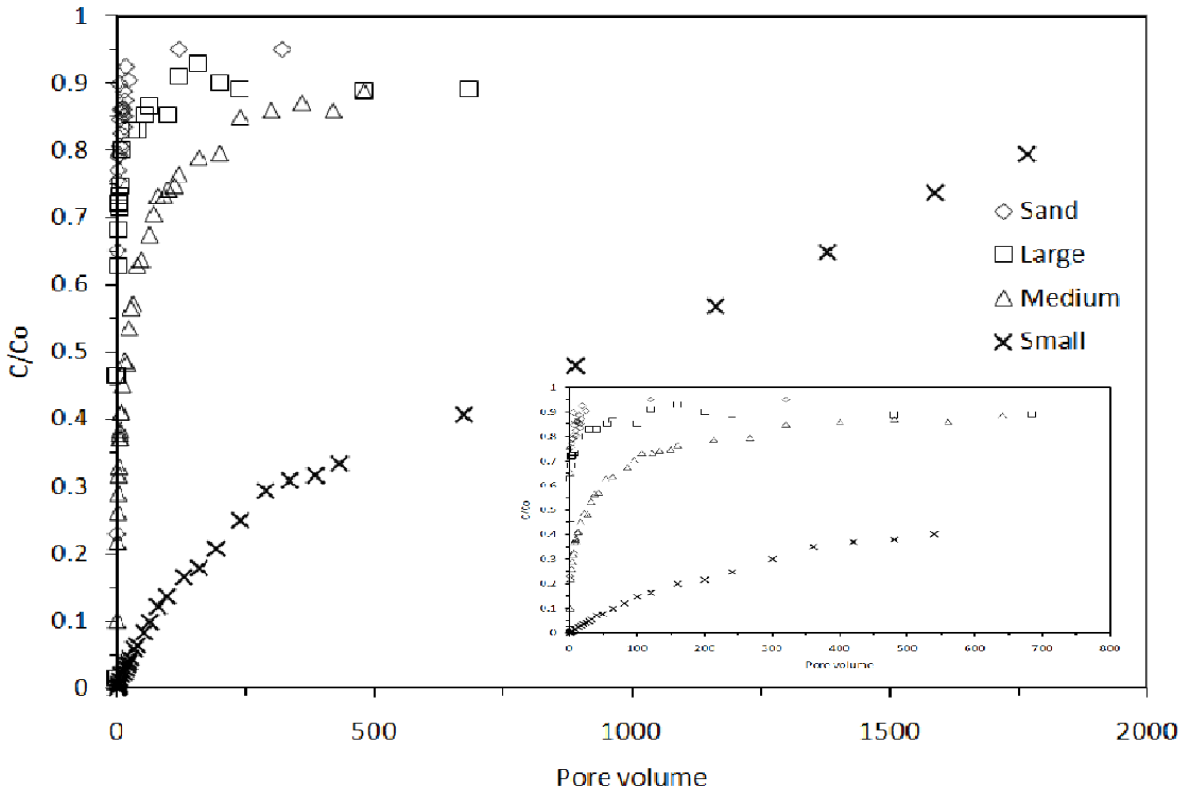

Figure 13: Column data- Effects of particle size on breakthrough concentrations(Experimental condition: influent U(VI) conc. 1 mg/L, CFHA 1.5 gm, 0.01 M $NaNO_3$, 0.01 M $NaHCO_3$, flow rate 10 ml/min, pH 8.5, and room temperature)

3.11 Effect of flow rate

Three column experiments were completed to study the influence of flow rate on uranium removal efficiency. Similar to the previous experiments, all the columns were filled with 1.5 grams of CFA and 7.5 grams of sand. The influent uranium concentration was 1 mg/L and the initial pH value was adjusted to 8.5. The influent pump was run at the following three distinct flow rates: 10 ml/min, 5 ml/min, and 2 ml/min. The breakthrough data from all three columns along with a control data (column packed with sand run with a flow rate of 5 ml/min) are shown in Figure 14. The results show that at the high flow rate (of 10 ml/min) the transport is influenced by kinetics and the overall breakthrough is spread over a wide range of time. On the other hand, the effluent breakthrough data from lower flow rates (of 2 and 5 ml/min) are almost same and the breakthrough pattern is relatively sharp.

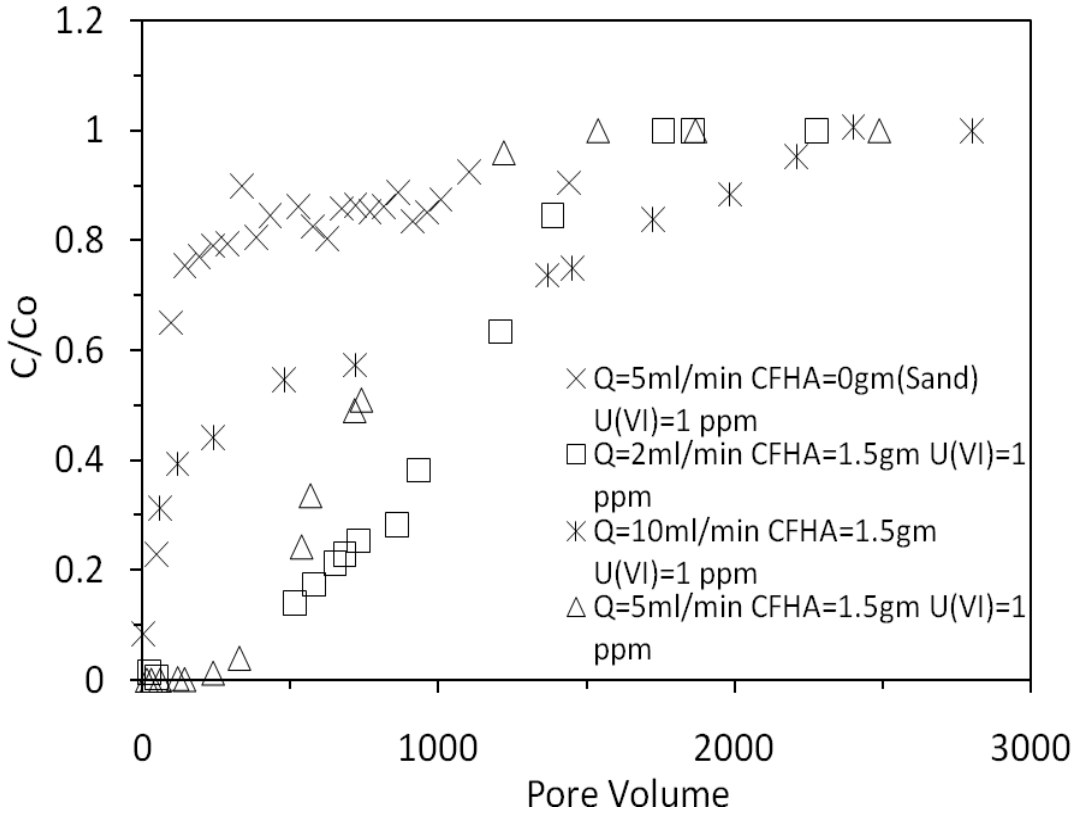

Figure 14: Column data- Effects of flow rates(Experimental condition: influent U(VI) conc. 1 mg/L, CFHA 1.5 gm, 0.01 M $NaNO_3$, 0.01 M $NaHCO_3$, pH 8.5, variable flow rates, and room temperature)

3.12 Testing the scalability of U(IV) removal processes

We hypothesized that under similar transport conditions, adsorption of uranium should exclusively depend on the amount of sorbent (CFHA) in the system and hence the performance of the column can be predicted based on the mass of the sorbent. In order to test this scaling hypothesis, we designed a column experiment with a flow rate of 5 ml/min, doubled the amount of CFHA in the system (to 3 grams) and simultaneously doubled the concentration of uranium in the influent solution. If our scaling hypothesis is true, then the effluent data from this experiment should be similar to the 5 ml/min data presented in figure 14. Figure 15 compares data from the two column experiments. The results show that both datasets are almost identical thus proving the adsorption of uranium onto CFHA to be a scalable process. The data also indicates that it took about 2400 pore volumes to fully breakthrough, when the effluent concentration was equal to the influent concentration. By integrating the area under the breakthrough curve, using the trapezoidal rule, we estimated that about 3.9 mg of uranium was removed by the column containing 1.5 grams of fish bone, which implies the fish bone material had a treatment capacity of 2.04 mg U (VI) / gm CFHA at pH value of 8.5, under dynamic transport conditions.

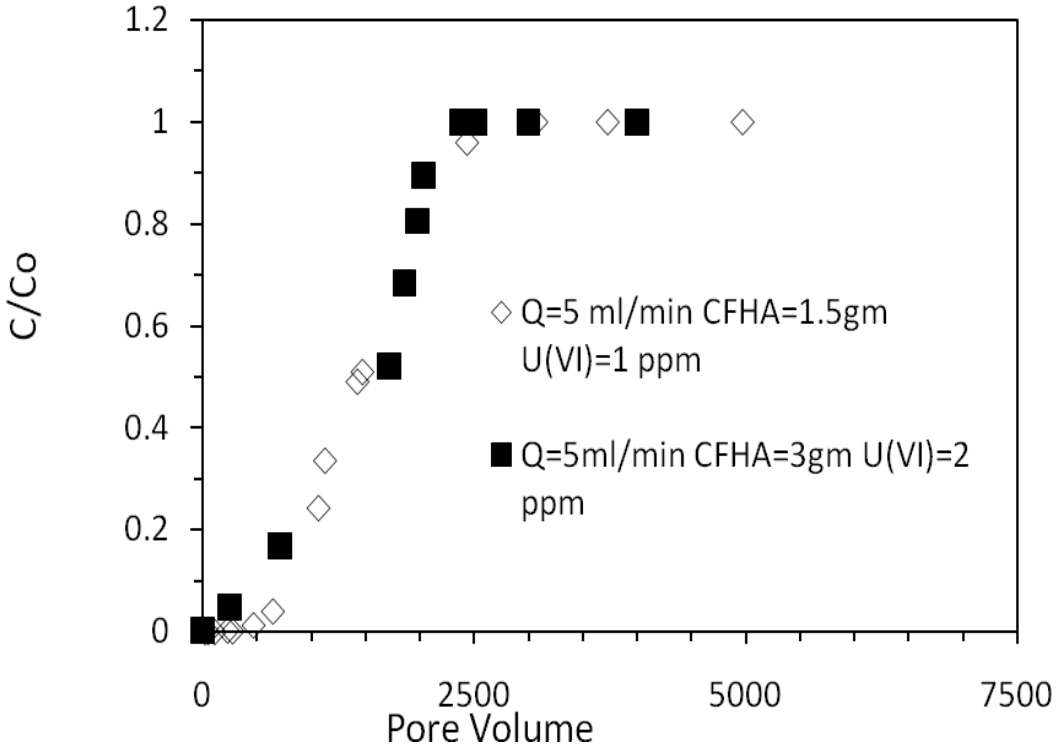

Figure 15: Scalability of observed breakthrough data at pH 8.5

(Experimental condition: Influent U(VI) concentration 1 and 2 mg/L, CFHA 1.5 and o3 g, 0.01 M $NaNO_3$, 0.01 M $NaHCO_3$, pH 8.5, flow rate 5 ml/min, and room temperature)

3.13 Column performance at pH 7

Batch data has already indicated that the removal capacity of the CFHA is higher at pH 7 when compared to its capacity at pH 8.5. We completed column experiments at pH 7 to test whether CFHA-containing columns could perform better when treating neutral pH waters containing dissolved uranium. In order to minimize the kinetic effect,

we also lowered the flow rate to 1 ml/ min to allow higher residence time in the column. Figure 16 provides the breakthrough data from a column containing 1.5 grams of FBHA treating 1 mg/L of uranium-contaminated water. The data show that it took about 2500 pore volumes to fully saturate the column (when the effluent concentration was equal to the influent concentration). By integrating the area under the breakthrough curve by using the trapezoidal rule, we estimated that the fish bone material had a treatment capacity of 3.9 mg U (VI) / gm CFHA at pH 7. This is approximately twice the value of the capacity observed at pH 8.5.

Mibus and Brendler 2005 conducted column experiments with commercial HAP and uranium stock solution. The column results indicated a retardation factor varying in the range of 27 to 45, for soils containing 0.1% of pure HA at a solution pH of 7.83. This column experiment done with 16% CFHA in our study showed a retardation factor of 2250 which is of the same magnitude as the value of retardation factor (4300) scaled from Mibus' results.

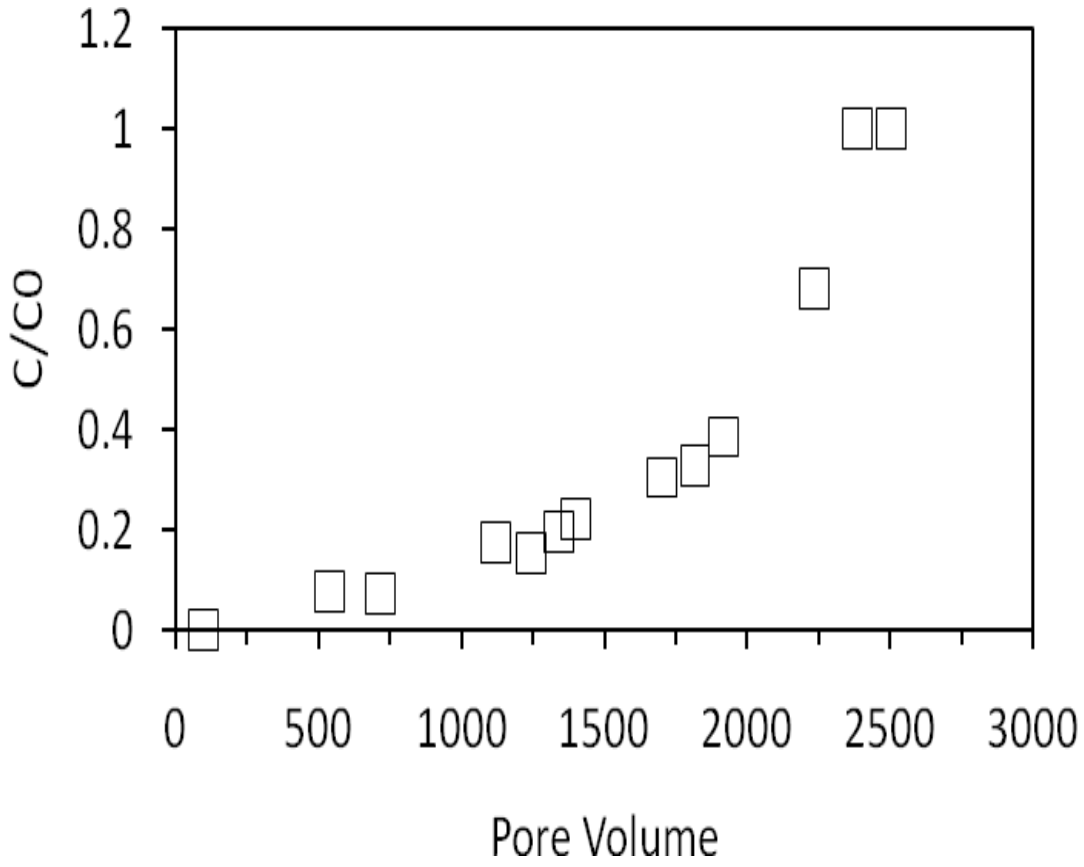

Figure 16: Break through data at pH 7 (Experimental condition: influent U(VI) concentration 1 mg/L, CFHA 1.5 g, 0.01 M $NaNO_3$, 0.01 M $NaHCO_3$, pH 7, flow rate 1 ml/min, and room temperature)

3.14 Verifying mass balance closure of batch and column data

The mass balance closure was checked independently by verifying the concentration of uranuim sequestered within the solid phase by digesting the batch- and column-derived solids with concentrated HNO_3 until the fish bone materials were

completely dissolved. Filtered digestate were then analyzed for uranium to evaluate the mass of uranium adsorbed onto the fish bone ($M_{measured}$).

We also computed the amount of mass lost from the aqueous phase to the solid phase using the measured aqueous phase concentration values. For batch experiments, we used the measured value of initial and final uranium aqueous concentrations to estimate the mass exchanged to the solid phase. For column experiments, the uranium mass attached to the solid phase was calculated by integrating (using trapezoidal rule) the total area under the C/Co vs time graph and multiplying this value with the flow rate to compute the amount of the amount of mass eluted from the system M_{eluted}. The total amount of mass supplied to the column was computed using: $M_{supplied} = QC_{inf}\ t_f$. The difference between these to two mass values provide a direct estimate of the mass sequested withi the column, which can be computed as: $M_{estimate} = M_{supplied} - M_{eluted}$.

For example, in Figure 15 (where we show column results for an experiment with 1.5 gm of CFHA to treat water containing 1 ppm uranium with a flow rate of 5 ml /min) the $M_{measured}$ for uranium was 2.76 mg. This value is very close to the graphically value of $M_{estimate}$ which was 3.06 mg. The mass balance error for this experiment was: 10.8%.

For the batch isotherm experiment reported in Figure 11, mass balance was done for a reactor used to develop the point corresponding to final uranium concentration of 2.1 mg/L (corresponding soild phase concentration of 8 mg/L). The results show the value of $M_{measured}$ was 0.4 mg and $M_{estimate}$ was 0.325 mg, and the corresponding mass balance error was about 18%.

CHAPTER 4

CONCLUSIONS AND RECOMMENDATIONS

There are numerous uranium contaminated sites in the world and remediation of these sites is a serious environmental challenge. For remediating uranium groundwater plumes there are only a few reactive adsorbents are available. Among these sorbents, natural hydroxyapatite is a special sorbent because it is inexpensive and efficient. In this study, remediation of uranium- contaminated groundwater by natural hydroxyapatite derived from catfish bones was investigated. Initially, pH edge experiments were completed for understanding the influence of the solution pH on uranium sorption. Uranium sorption onto CFHA was maximum near neutral pH conditions (5-8.5). Batch isotherm experiments were completed using CFHA at different pH values. The results showed a maximum sorption capacity at pH 7 is about 18 mg of U/g CFHA.

Batch kinetic studies were completed using CFHA prepared at two different temperatures (100°C & 300°C) to understand the effect of preparation temperature on uranium sorption. The CFHA heated at lower temperature (100°C) was found to be more efficient due to its higher surface area inferred which was from the SEM images. Therefore, CFHA particles prepared at 100°C were used in all subsequent studies.

To investigate the effect of particle size of CFHA on uranium removal, the CFHA particles were crushed and segregated into three different categories: large (>2000μ), medium (between 2000 μ and 300 μ) and small (<300 μ). Both batch and column experiments were completed to study the effect of particle size on uranium sequestration. The column data show that breakthough occurred around 1, 22, 880 pore volumes, for columns with large, medium, and small particles, respectively. The results indicated that the smaller particles have the highest sorption efficiency, and the largest particles have the least sorption efficiency. This is attributed to the availability of higher surface area in the smaller particles, which enhances surface sorption of uranium.

A series of column experiments were completed to study the effect of seepage velocity on uranium removal by using three different flow rates (10, 5, 2 ml/min). The results showed that at higher flow rates (10 ml/min) the transport was influenced by kinetic effects; whereas at 5 and 2 ml/min the breakthrough profiles were almost identical, indicating the minimal kinetic effects.

Under similar transport conditions, adsorption of uranium would depend on the amount of sorbent (CFHA) in the system and hence the performance of the column could be scaled based on the mass of the sorbent. To test this hypothesis, column experiments were designed to treat 1 and 2 mg/L of uranium solution with column containing 1.5 and 3 mg of CFHA. The breakthroughs profile observed from these two experiments were nearly identical indicating that the adsorption process is scalable. Finally, mass balance verifications were done for both batch and column datasets to confirm that uranium is lost

only to the CFHA particles. For batch experiments, the mass balance error was about 20% and for column experiments it was about 10%.

Recommendations

When the CFHA particles were heated at very high temperatures (550°C) for a long duration they became charred. This charring has an interesting effect on uranium sequestration. It not only increased the sorption capacity, but also appears to improve the kinetics (see Appendix-II for data). A comparison of the uranium removal efficiency of CFHA charred at different temperatures will be an useful follow up research effort. Furthermore, uranium removal processes in PRBs can be studied by using physical laboratory models or pilot-scale field experiments.

REFERENCES

Admassu W, Breese T. Feasibility of using natural fishbone apatite as a substitute for hydroxyapatite in remediating aqueous heavy metals. Journal of Hazardous Materials 1999; 69: 187-196.

Akira Tashiro,Discounted Casualties, 2001**:** The Human Cost of Depleted Uranium http://www.xs4all.nl/%7Estgvisie/VISIE/du-diagnosis-txt.html

Arey JS, Seaman JC, Bertsch PM. Immobilization of Uranium in Contaminated Sediments by Hydroxyapatite Addition. Environ Sci Technol 1999; 33: 337-342.

Argonne National Laboratory, (USDOE), 2009, http://web.ead.anl.gov/uranium/guide/ucompound/health/index.cfm

Babu MNS, Somashekar RK, Kumar SA, Shivanna K, Krishnamurthy V, Eappen KP. Concentration of uranium levels in groundwater. International Journal 2008; 5: 263-266.

BBC, 2009, http://www.bbc.co.uk/schools/gcsebitesize/maths/shapes/3dshapesrev3.shtml

Biltz RM, Pellegri.Ed. Chemical Anatomy of Bone .I. a Comparative Study of Bone Composition in 16 Vertebrates. Journal of Bone and Joint Surgery-American Volume 1969; A 51: 456-466.

Chen XB, Wright JV, Conca JL, Peurrung LM. Effects of pH on heavy metal sorption on mineral apatite. Environmental Science & Technology 1997; 31: 624-631.Cheng T, Barnett MO, Roden EE, Zhuang J. Effects of Phosphate on Uranium(VI) Adsorption to Goethite-Coated Sand. Environ Sci Technol 2004; 38: 6059-6065.

Cheng T, Barnett MO, Roden EE, Zhuang J. Effects of Solid-to-Solution Ratio on Uranium(VI) Adsorption and Its Implications. Environ Sci Technol 2006; 40: 3243-3247.

Conca JL, Wright J. An apatite II permeable reactive barrier to remediate groundwater containing Zn, Pb and Cd (vol 21, pg 1288, 2006). Applied Geochemistry 2006; 21: 2187-2200.

Cooper JJ. Bone for bone china. British ceramic transactions 1995; 94: 165-168.

Deb S, Giri J, Dasgupta S, Datta D, Bahadur D. Synthesis and characterization of biocompatible hydroxyapatite coated ferrite. Bulletin of Materials Science 2003; 26: 655-660.

del Rio JG, Sanchez P, Morando PJ, Cicerone DS. Retention of Cd, Zn and Co on hydroxyapatite filters. Chemosphere 2006; 64: 1015-1020.

EIA, 2006, http://www.eia.doe.gov/cneaf/nuclear/page/at_a_glance/states/statesaz.html

Fernane F, Mecherri MO, Sharrock P, Hadioui M, Lounici H, Fedoroff M. Sorption of cadmium and copper ions on natural and synthetic hydroxylapatite particles. Materials Characterization 2008; 59: 554-559.

Fetter CW. Applied Hydrogeology, 1988. In: Merrill Publishing Co., Columbus, Ohio.

Fuller CC, Bargar JR, Davis JA, Piana MJ. Mechanisms of Uranium Interactions with Hydroxyapatite: Implications for Groundwater Remediation. Environ Sci Technol 2002; 36: 158-165.

Fuller CC, Bargar JR, Davis JA. Molecular-scale characterization of uranium sorption by bone apatite materials for a permeable reactive barrier demonstration. Environmental Science & Technology 2003; 37: 4642-4649.

Giammar DE, Hering JG. Time scales for sorption-desorption and surface precipitation of uranyl on goethite. Environmental Science & Technology 2001; 35: 3332-3337.

Giammar DE, Xie LY, Pasteris JD. Immobilization of lead with nanocrystalline carbonated apatite present in fish bone. Environmental Engineering Science 2008; 25: 725-735.

Giammarand D, Hering J. Time scales for sorption-desorption and surface precipitation of uranyl on goethite. 2001; 35: 3332-3337.

Glimcher MJ. Molecular Biology of Mineralized Tissues with Particular Reference to Bone. Rev Mod Phys 1959; 31: 359-393.

Grenthe I, Wanner H, Forest I, Agency ONE. Chemical thermodynamics of uranium. North-Holland Amsterdam, 1992.

Hamada M, Nagai T, Kai N, Tanoue Y, Mae H, Hashimoto M, Miyoshi K, Kumagai H, Saeki K. Inorganic constituents of bone of fish. Fisheries Science (Japan) 1995;

Han RP, Zou WH, Wang Y, Zhu L. Removal of uranium(VI) from aqueous solutions by manganese oxide coated zeolite: discussion of adsorption isotherms and pH effect. Journal of Environmental Radioactivity 2007; 93: 127-143.

Hettiarachchi GM, Pierzynski GM. Soil lead bioavailability and in situ remediation of lead-contaminated soils: A review. Environmental Progress 2004; 23: 78-93.

Hwang A, Ji W, Khim J. Characteristics of phosphorus containing waste-bones. Materials Letters 2007; 61: 677-679.

Jerden JL, Sinha AK. Phosphate based immobilization of uranium in an oxidizing bedrock aquifer. Applied Geochemistry 2003; 18: 823-843.

Jones AP, Wall F, Williams CT. Rare earth minerals: chemistry, origin and ore deposits. Kluwer Academic Publishers, 1996.

Joye JL, Naftz DL, Davis JA, Frethey GW, Rowland RC. Handbook of Groundwater remedaition using permeable reactive barriers. 2002; 195-219.

Koeppenkastrop D, De Carlo EH. Sorption of rare-earth elements from seawater onto synthetic mineral particles: An experimental approach. Chemical geology 1992; 95: 251-263.

Kong LB, Ma J, Boey F. Nanosized hydroxyapatite powders derived from coprecipitation process. Journal of Materials Science 2002; 37: 1131-1134.

Korte NE, Fernando Q. A review of arsenic (III) in groundwater. . Critical Review of Environmental Control 1991; 21: 1-39.

Krestou A, Xenidis A, Panias D. Mechanism of aqueous uranium (VI) uptake by hydroxyapatite. Materials engineering 2004; 17: 373-381.

Liu HS, Chin TS, Lai LS, Chiu SY, Chung KH, Chang CS, Lui MT. Hydroxyapatite synthesized by a simplified hydrothermal method. Ceramics International 1997; 23: 19-25.

Ma QY, Traina SJ, Logan TJ, Ryan JA. In-Situ Lead Immobilization by Apatite. Environmental Science & Technology 1993; 27: 1803-1810.

Manecki M, Maurice PA, Traina SJ. Kinetics of aqueous Pb reaction with apatites. Soil Science 2000; 165: 920-933.

Martin WA, Larson SL, Felt DR, Wright J, Griggs CS, Thompson M, Conca JL, Nestler CC. The effect of organics on lead sorption onto Apatite II (TM). Applied Geochemistry 2008; 23: 34-43.

McDiarmid MA. Depleted uranium and public health - Fifty years' study of occupational exposure provides little evidence of cancer. Br Med J 2001; 322: 123-124.

Mibus J, Brendler V. Interaction of uranium from seepage water with hydroxyapatite. Uranium in the Environment: Mining Impact And Consequences 2005; 359.

Moore RC, Gasser M, Awwad N, Holt KC, Salas FM, Hasan A, Hasan MA, Zhao H, Sanchez CA. Sorption of plutonium (VI) by hydroxyapatite. In: Lausanne: Elsevier Sequoia,[1984-, 2005, 97-101.

Morrison SJ, Spangler RR. Extraction of Uranium and Molybdenum from Aqueous-Solutions - a Survey of Industrial Materials for Use in Chemical Barriers for Uranium Mill Tailings Remediation. Environmental Science & Technology 1992; 26: 1922-1931.

NAVFAC, 2009, https://portal.navfac.navy.mil/portal/page/portal/NAVFAC/NAVFAC_WW_PP/NAVFAC_NFESC_PP/ENVIRONMENTAL/ERB/PRB

Nriagu JO. Lead Orthophosphates .4. Formation and Stability in Environment. Geochimica Et Cosmochimica Acta 1974; 38: 887-898.

Ohnuki T, Kozai N, Samadfam M, Yasuda R, Yamamoto S, Narumi K, Naramoto H, Murakami T. The formation of autunite (Ca (UO2) 2 (PO4) 2nH2O) within the leached layer of dissolving apatite: incorporation mechanism of uranium by apatite. Chemical Geology 2004; 211: 1-14.

Ozawa M, Suzuki S. Microstructural development of natural hydroxyapatite originated from fish-bone waste through heat treatment. Journal of the American Ceramic Society 2002; 85: 1315-1317.

Ozawa M, Kanahara S. Removal of aqueous lead by fish-bone waste hydroxyapatite powder. Journal of Materials Science 2005; 40: 1037-1038.

Phillips DH, Gu B, Watson DB, Parmele CS. Uranium removal from contaminated groundwater by synthetic resins. Water Research 2008; 42: 260-268.

Raicevic S, Wright JV, Veljkovic V, Conca JL. Theoretical stability assessment of uranyl phosphates and apatites: Selection of amendments for in situ remediation of uranium. Science of The Total Environment 2006; 355: 13-24.

Rakovan J, Reeder RJ, Elzinga EJ, Cherniak DJ, Tait CD, Morris DE. Structural characterization of U(VI) in apatite by X-ray absorption spectroscopy. Environmental Science & Technology 2002; 36: 3114-3117.

Roehl KE, Simon FG, Meggyes T, Czurda K. Improvements in long-term performance of permeable reactive barriers. Geotechnical and Environmental Aspects of Waste Disposal Sites 2006; 163.

Saxena S, Prasad M, D'Souza SF. Radionuclide sorption onto low-cost mineral adsorbent. Industrial & Engineering Chemistry Research 2006; 45: 9122-9128.

Seaman JC, Meehan T, Bertsch PM. Immobilization of cesium-137 and uranium in contaminated sediments using soil amendments. Journal of Environmental Quality 2001; 30: 1206-1213.

Simon FG, Biermann V, Peplinski B. Uranium removal from groundwater using hydroxyapatite. Applied Geochemistry 2008; 23: 2137-2145.

Skinner HCW. Low temperature carbonate phosphate materials or the carbonate apatite problem: a review. Origin, evolution and modern aspects of biomineralization in plants and animals, Plenum Press, New York 1989, 251–264 pp.

Tang RK, Wang LJ, Nancollas GH. Size-effects in the dissolution of hydroxyapatite: an understanding of biological demineralization. Journal of Materials Chemistry 2004; 14: 2341-2346.

Thakur P, Moore RC, Choppin GR. Sorption of U(VI) species on hydroxyapatite. Radiochimica Acta 2005; 93: 385-391.

Thomson BM, Smith CL, Busch RD, Siegel MD, Baldwin C. Removal of metals and radionuclides using apatite and other natural sorbents. Journal of Environmental Engineering-Asce 2003; 129: 492-499.

Ulusoy U, Akkaya R. Adsorptive features of polyacrylamide–apatite composite for Pb2+, UO22+ and Th4+. Journal of Hazardous Materials 2009; 163: 98-108.

USEPA, 2004, http://www.epa.gov/fedrgstr/EPA-WATER/2004/June/Day-02/w12300.htm

USGS, 1995, http://energy.cr.usgs.gov/other/uranium/more.html

Wellman DM, Glovack JN, Parker K, Richards EL, Pierce EM. Sequestration and retention of uranium(VI) in the presence of hydroxylapatite under dynamic geochemical conditions. Environmental Chemistry 2008; 5: 40-50.

Wiki pedía, 2009, http://en.wikipedia.org/wiki/Hydroxyapatite

Wright J, Rice KR, Murphy B, Conca J. PIMS Using APATITE II™: How It Works To Remediate Soil & Water. Sustainable Range Management(Eds) RE Hinchee and B Alleman Battelle Press, Columbus, OH www batelle org/bookstore, ISBN 2004; 1-57477.

WSWS, James Conachy, 9 September 2003, http://www.xs4all.nl/~stgvisie/VISIE/du-diagnosis.html

Wu LM, Forsling W, Schindler PW. surface complexation of calcium minerals in aqueous-solution .1. surface protonation at fluorapatite water interfaces. Journal of Colloid and Interface Science 1991; 147: 178-185.

Yahoo education, 2005, http://education.yahoo.com/homework_help/math_help/problem?id=mini6and7gt_7_1_1_19_60

Yamashita K, Kanazawa T. Inorganic Phosphate Materials, 1989, edit T. Kanazawa (Elsevier Science, Tokyo, Japan, 1989) p 24-70.

Zhang H, Yang C, Tao Z. Effects of phosphate and fulvic acid on the sorption and transport of uranium (VI) on silica column. Journal of Radioanalytical and Nuclear Chemistry 2009; 279: 317-323.

Zhang H, Tang Q, Tao Z. Effects of phosphate and Cr 3+ on the sorption and transport of uranium (VI) on a silica column. Journal of Radioanalytical and Nuclear Chemistry 2009; 279: 855-861.

APPENDIX – I

Microscope Images

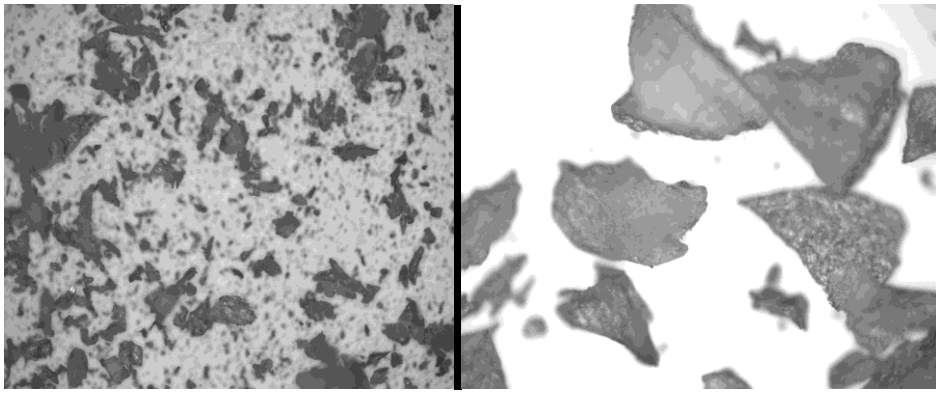

Figure A1-1: Optical microscopic images of catfish bones heated at 100 ℃ and **300**℃ **respectively at 300µ level**

Figure A1-2: Treating the catfish bone wastes by pressure cooking

Figure A1-3: Flesh removal from catfish wastes by hand

Figure A1-4: CFHA after chemically treating with hydrogen peroxide

APPENDIX – II

Figures:

Figure A2-1: Image of fish bone heated at 550°C (Charred CFHA)

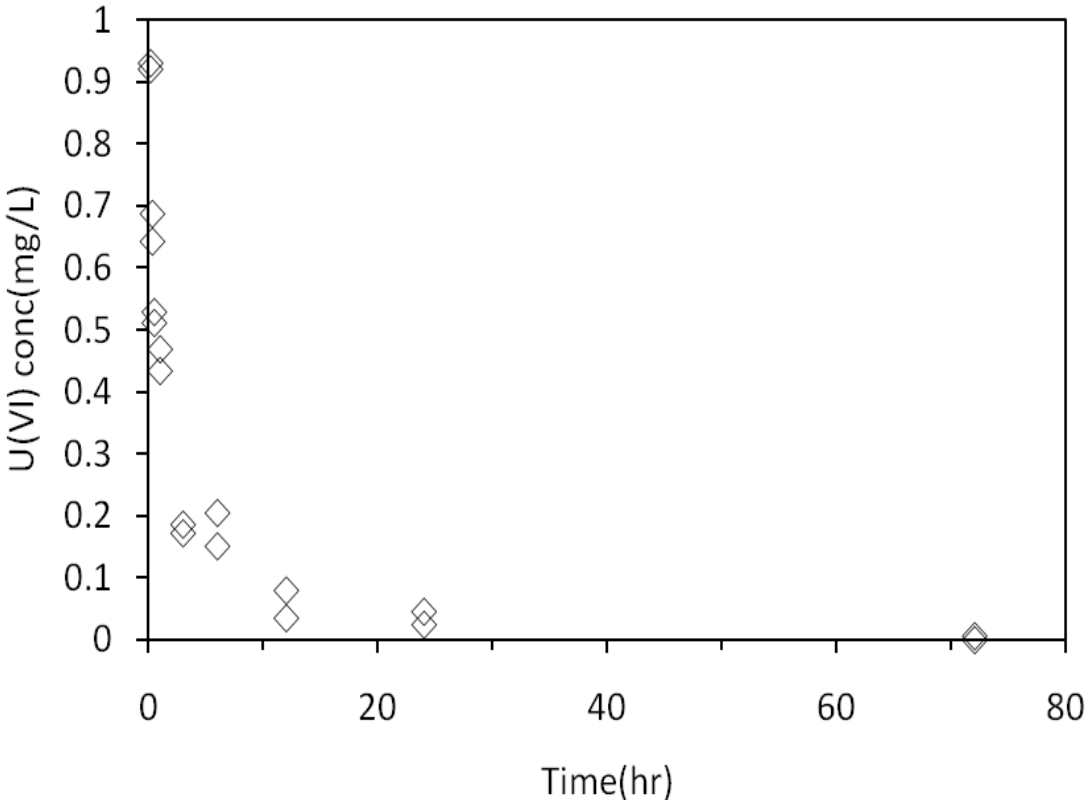

Figure A2-2: Batch Kinetic experiment for CFHA prepared at 550 ℃

(Experimental conditions: 1 mg/L of initial U(VI), 0.5 g/L of CFHA, 0.01 M NaNO3, 0.01 M NaHCO3, pH 7 and room temperature)